Deliverable Tasks 5.0b & 6.0c

Statistical Analysis of Sixteen Years of Water Quality Data Project

Final Report

Report to the Elkhorn Slough Foundation and
the Community Foundation for Monterey County

Prepared by the University of California at Santa Cruz

November 5, 2008

Acknowledgements

Funding for this research was provided in part by the Community Foundation of Monterey County and the Elkhorn Slough Foundation, through a donor-advised fund with the Central Coast Regional Water Quality Control Board.

The authors acknowledge the hard work of Sue Shaw who as faithfully collected the water samples since 1988 as a volunteer and to the Elkhorn Slough staff who have increased the data quality and quantity, but also have provide extremely valuable insight to interpret the results for this manuscript.

Table of Contents

Table of Tables

Table of Figures

Executive Summary

We analyzed water quality parameters to determine whether long-trends are occurring in 16 years of water quality data in Elkhorn Slough. In spite of the numerous data quality issues, e.g. changing methods, missing data, and the hydrological complexity, we found significant trends throughout the slough with various measures. We report the use of parametric and non-parametric methods in this report and, in some cases, are able to compare the results.

Water quality within Elkhorn Slough varies on both temporal and spatial scales. The trends at individual sites provide resounding support that monitoring water quality is a sensitive method of tracking ecosystem health. The source of variability, increasing turbidity, and elevated nutrient concentrations remains unknown. Numerous anthropogenic changes have influenced the Elkhorn Slough watershed; however, the long-term effects are difficult to ascertain. More monitoring is needed to link water quality parameters and ecosystem health in this complex system.

Introduction

Estuaries are the most highly impacted habitat types by humans, yet these habitats host rich, distinctive biodiversity, including migratory shorebirds, and nursery fishes, among others (Edgar et al. 2000). Even though Elkhorn Slough is a small, shallow estuary on a national scale, it is the largest estuary along a 230 mile stretch of coastline between San Francisco and Morro Bay, California USA. It has an extremely important ecological role within a variety of habitats, including extensive marshes and mudflats. Each estuary has unique, often complicated, spatial and temporal characteristics. Therefore, it is a challenge to develop and maintain monitoring programs to capture this variability while developing record lengths long enough to discern water quality trends amid seasonal variation.

One of the goals of the Elkhorn Slough National Estuarine Research Reserve (ESNERR) is to examine spatial and temporal variation water quality and nutrient concentrations to assess changes in ecosystem status of the whole estuary at the site-specific level. Under that scope, we considered if there were significant long-term trends during the period 1988-2004 and if these changes occur similarly across the reserve, or some regions present stronger signals. We examined records from 24 sites in the ESNERR where the collection monthly water quality data occurred for as long as 16 years.

Site Description

Elkhorn Slough is located in the Monterey Bay area, between the cities of Watsonville and Salinas, along the central coast of California with a mild, Mediterranean climate. Elkhorn Slough is part of the National Estuarine Research Reserve (NERR) system. It plays an extremely important ecological role with a variety of habitats including extensive marshes and mudflats, which are rare along the central coast of California. Intertidal mudflats with broad mats of macroalgae and pickleweed marsh (*Salicornia virginica*) border the main channel and tidal creeks. The slough is rich biologically with approximately 800 species of invertebrates, 500 species of plants, 80 species of fish, 30 species of reptiles and amphibians, 50 species of mammals, and 200 species birds.. Air temperature and rainfall vary on a seasonal basis (ESNERR unpublished data).

The hydrology of Elkhorn Slough has changed dramatically since the 1880s. Historically, the slough was a network of interconnected estuarine arms and perennial freshwater sources. Berms, culverts and tidal gates have cut off tidal flow to many portions of the slough. The Old Salinas River channel; Moro Cojo, Tembladero, and Bennett Sloughs; and upper margins of Elkhorn main channel (Porter Marsh, North Marsh) receive little to no tidal flow (varies by site). In contrast, the main channel of the slough, artificially opened to allow vessels, no longer functions as a backwater, stagnant waterway. The slough experiences semi-diurnal tidal action. Water in the lower portion of the slough and harbor has a residence time less than one day, while water in the northern portion of the main channel has longer residence time, with a large range between 1 and 50 days depending on the freshwater inputs (Largier 1997; Caffrey

2007). Finally, surface water and groundwater extractions have reduced freshwater sources and altered habitat types. Currently, the main channel extends inland for 11.4 kilometers (km) from Monterey Bay. It receives seawater exchanges through the mouth and terrestrial freshwater from the Salinas River, an assortment of small creeks and runoff from local terrestrial sources. Some areas have limited tidal exchange and water quality is subject to adjacent land uses, while other areas have extremely high flows with have marine dominated waters.

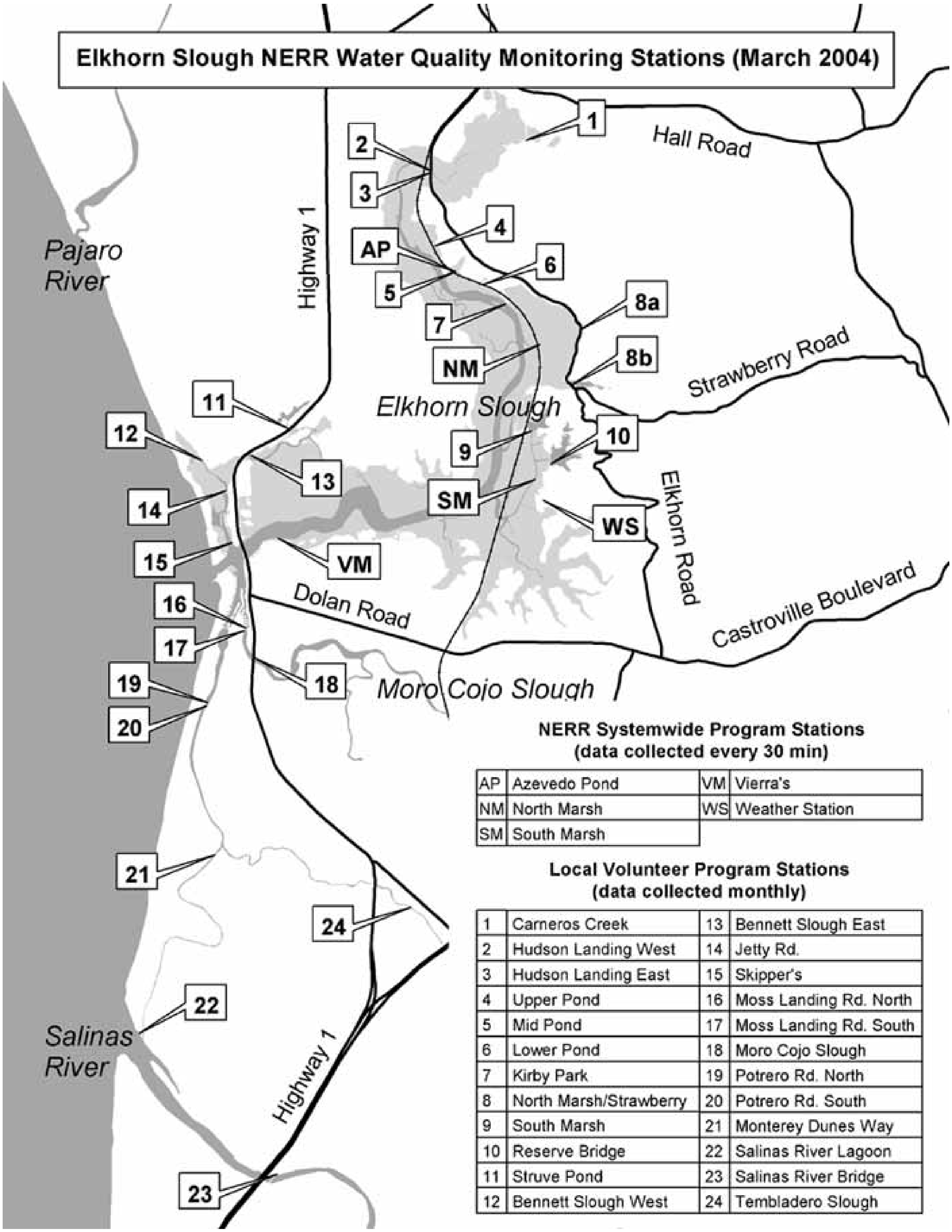

AP	Azevedo Pond	VM	Vierra's
NM	North Marsh	WS	Weather Station
SM	South Marsh		

1	Carneros Creek	13	Bennett Slough East
2	Hudson Landing West	14	Jetty Rd.
3	Hudson Landing East	15	Skipper's
4	Upper Pond	16	Moss Landing Rd. North
5	Mid Pond	17	Moss Landing Rd. South
6	Lower Pond	18	Moro Cojo Slough
7	Kirby Park	19	Potrero Rd. North
8	North Marsh/Strawberry	20	Potrero Rd. South
9	South Marsh	21	Monterey Dunes Way
10	Reserve Bridge	22	Salinas River Lagoon
11	Struve Pond	23	Salinas River Bridge
12	Bennett Slough West	24	Tembladero Slough

Figure 1. Water quality sampling locations sites (courtesy of the Elkhorn Slough Foundation).

Beginning in the 1700s, land was cleared for agriculture, and by the 1880s significant loss of upland topsoils had resulted in sedimentation of many wetland areas. With the construction of dikes and berms, wetlands were either drained for grazing and agriculture or ponded for hunting. These activities dominated the slough through the 1960s. In the 1970s, pastures and dairies were the dominant agricultural land use. By the 1990s, many of these lands were converted to agricultural row crops both along flat areas next to the Slough as well as steep hill slopes (Van Dyke and Wasson 2005). Row crops such as strawberries, flowers, artichokes, and raspberries dominate current agricultural land use and occur on approximately 24% of the watershed. Most of the land is zoned rural residential, with a majority of the homes using septic systems. Urban and commercial land uses represent about 16% of the land cover and are concentrated in the towns of Moss Landing and Castroville. Managed in its natural state by a variety of state and federal agencies, or private non-profit organizations approximately 14% of the watershed is protected (Van Dyke & Wasson, 2005). More information about Elkhorn Slough is available from http://www.elkhornslough.org/.

Water Quality Monitoring Program

The data considered in this paper are the result of a 16-year program carried out by a combination of volunteers and professional support. Starting in the fall of 1988, several stations in the Elkhorn Slough were sampled on a monthly basis for temperature, salinity, pH, turbidity, dissolved oxygen, ammonium, nitrate, and soluble reactive phosphorous. The number of stations increased over time, from 6 to 24. Depth of sample collection varied between 0.05 to 0.5 meters depending on water level and flow. Volunteers collected both in-situ and grab samples for laboratory nutrient analyses and volunteers have remained remarkably consistent and dedicated since 1988.

From 1988-1994, conductivity, salinity and temperature were measured in situ using a YSI 33 (Yellow Springs, OH) sonde. Dissolved oxygen was measured using a YSI 57, pH was measured using an Orion 211 pH meter and turbidity was measured using a Moniteck 21 PE turbidity meter. In late 1994, the program switched to using a Solomat 803PS (Norwalk, Connecticut) to measure temperature, pH, salinity/conductivity, dissolved oxygen, and turbidity. From 2000-present, a YSI 6000 (Yellow Springs, OH) multi-parameter water quality sonde was used to measure conductivity (converted to practical salinity units), temperature, pH, dissolved oxygen, turbidity and depth. All instruments were calibrated according to their respective manual instructions.

Water samples were collected into brown polypropylene or polyethylene bottles and transported to the laboratory in the dark on ice. Samples were filtered within 48 hours of collection. From 1989-1991, nutrient analyses were performed by the Monterey Bay Aquarium using standard wet chemical techniques for NO_3^-, NH_4^+, and PO_4^3 (Apkem Series 300, OI Analytical, College Station, TX). Starting in December 1991 to present, nutrients were analyzed at the Monterey County Consolidated Chemistry Laboratory (MCCCL) using standard methods ((APHA) 1985). Currently, method EPS350.3 is used for NH_4-N, EPA300 is used for NO_3, and SM4500PE is used for PO_4-P.

Exploratory Analysis

We performed a detailed exploratory analysis, at the onset of each analysis. We used probability plots to estimate values below laboratory detection limits that followed non-parameter distributions (Helsel and Hirsch 1992). The open source software R (CRAN 2008) reported summary statistics including distribution-free confidence intervals and medians. To explore site-specific, long-term trends, we used the seasonal Kendall test. This distribution free (non-parametric) test partitions data into seasonal categories (Helsel and Hirsch 1992). In this case, we used month as the season (i.e., 12 seasons per year). We ran the tests twice for each site and parameter because of changing laboratory methods (and detection limits). We assumed values below the detection limit were zero, then assumed values below the detection limit were equal to the detection limit.

Description of the Spatial Patterns

Water parameters varied dramatically spatially within the slough. Most water quality parameters had highly skewed distributions, and nutrients concentrations were often outside the 95% distribution-free confidence intervals of the median. We report both mean and median but used median as a more robust measure of site water quality characteristics. Water temperatures ranged from 2 to 33^{o} C (Table 1). Median temperatures were lowest near the mouth of the slough and generally increased with distance from the mouth. The warmest temperatures occurred at the northern part of the slough in the three Azevedo ponds. Salinity concentrations ranged from -0.12 to 89 ppt. Salinity was generally lowest at locations where freshwater enter the slough at the north, near Carneros Creek and south near the Salinas River (Table 2). The Azevedo Ponds, Struve Pond, and Strawberry Road, reached very high salinities in during the warm and dry months of July, August and September. The pH medians ranged from 7.95 to 8.65. The lowest pH was in Carneros Creek while the highest occurred in Salinas River at Highway 1 and in Tembladero Slough (Table 3). Daytime median dissolved oxygen (DO) concentrations were between 7.4 and 11.76 mg/L (Table 4). The highest water column DO concentrations were found in the Salinas River at Highway 1, and the lowest generally occurred at South Marsh and Reserve Bridge. Turbidity median ranged from 5 to 73.2 NTUs and were highest in sites with low flushing and adjacent farmland (Table 5). Turbidity was generally lowest in the sites near the main channel.

Table 1. Temperature: Mean, Median, Distribution Free 95% Confidence Interval, and Trend (Seasonal Kendall test).

Site	N	mean	skew	median	95% CI		Trend
1	153	17.13	-0.09	17.5	16.6	18	NS
2	161	18.27	-0.21	18.62	18	19.4	$+ 0.15^{o}c\ yr^{-1}$ ($p < 0.01$)
3	162	18.10	-0.11	18.5	17.8	19.26	$+ 0.19^{o}c\ yr^{-1}$ ($p < 0.01$)
4	129	18.78	0.37	18.59	17.2	19.5	NS
5	108	19.20	-0.01	19.36	17.8	20.81	$+ 0.45^{o}c\ yr^{-1}$ ($p < 0.01$)
6	128	20.11	0.11	19.75	18.9	21.2	$+ 0.33^{o}c\ yr^{-1}$ ($p < 0.001$)
7	164	16.76	-0.17	16.99	16.2	17.74	NS
8	67	20.25	-0.14	19.7	18.3	22.07	NS
8.5	93	17.96	-0.24	18	17	19.2	NS
9	159	17.20	-0.13	17.6	16.8	18.2	$+ 0.11^{o}c\ yr^{-1}$ ($p < 0.01$)
10	160	16.33	-0.19	16.76	16	17.54	$+ 0.14^{o}c\ yr^{-1}$ ($p < 0.01$)
11	171	17.77	-0.03	18.2	16.9	19.1	NS
12	170	17.03	0.10	16.9	16.2	17.77	NS
13	153	17.15	-0.34	17.56	16.8	18.36	$+ 0.1^{o}c\ yr^{-1}$ ($p < 0.05$)
14	175	16.51	0.22	16.5	15.8	17.05	NS
15	187	15.41	0.69	15.2	14.8	15.5	$+ 0.17^{o}c\ yr^{-1}$ ($p < 0.001$)
16	147	16.26	0.13	16.2	15.6	16.8	$+ 0.09^{o}c\ yr^{-1}$ ($p < 0.05$)
17	147	16.83	0.09	16.8	16.2	17.4	$+ 0.15^{o}c\ yr^{-1}$ ($p < 0.05$)
18	175	17.96	-0.17	18.21	17.2	18.93	NS
19	162	16.30	-0.09	16.595	16	17	$+ 0.07^{o}c\ yr^{-1}$ ($p < 0.05$)
20	163	17.47	-0.03	17.2	16.2	18.41	NS
21	137	17.11	0.05	17.5	16.2	18.29	NS
22	99	16.24	-0.24	16.7	15.3	17.6	$+ 0.34^{o}c\ yr^{-1}$ ($p < 0.05$)
23	161	17.12	-0.34	17.99	16.6	18.88	$+ 0.12^{o}c\ yr^{-1}$ ($p < 0.01$)
24	106	16.81	-0.53	17.1	16.3	18.5	NS

Table 2. Salinity: Mean, Median, Distribution Free 95% Confidence Interval, and Trend (Seasonal Kendall test).

Site	N	mean	skew	median	95% CI		trend
1	153	10.8	0.9	3.3	2.1	7.3	= - 0.65 ppt/yr (p < 0.001)
2	162	26.3	-0.9	29.6	27.4	31.0	NS
3	163	22.2	-0.5	25.0	22.0	28.1	= - 0.56 ppt/yr (p < 0.01)
4	133	28.7	-1.7	31.6	30.3	32.3	NS
5	105	26.9	1.0	23.9	19.0	31.5	= + 1.86 ppt/yr (p < 0.001)
6	132	30.5	0.3	29.1	24.0	36.0	NS
7	168	29.2	-1.8	31.9	31.0	32.5	= + 0.14 ppt/yr (p < 0.05)
8	69	35.9	-0.2	35.9	30.5	42.1	NS
8.5	95	28.8	-0.7	30.0	28.0	32.5	NS
9	161	30.1	-1.9	31.9	31.2	32.3	= + 0.19 ppt/yr (p < 0.01)
10	163	29.3	-1.7	31.5	30.8	32.1	NS
11	173	29.1	-0.1	31.5	27.4	34.2	= + 0.42 ppt/yr (p < 0.05)
12	174	27.9	-1.8	31.3	30.6	31.9	NS
13	149	28.9	-0.9	31.5	30.1	32.5	NS
14	180	28.8	-1.8	31.3	30.5	31.8	NS
15	192	29.2	-1.9	31.5	31.1	32.0	NS
16	152	24.2	-1.1	27.3	26.1	28.2	= - 0.38 ppt/yr (p < 0.05)
17	149	22.9	-0.7	29.0	26.0	30.0	NS
18	179	25.3	-0.6	30.5	28.0	31.6	= - 0.24 ppt/yr (p < 0.05)
19	166	17.0	-0.1	18.5	13.9	21.0	= - 0.59 ppt/yr (p < 0.01)
20	165	7.1	1.6	5.0	4.0	6.2	NS
21	140	6.5	1.9	5.1	3.7	6.1	= - 0.33 ppt/yr (p < 0.01)
22	103	9.1	1.7	6.0	5.0	7.9	= - 0.59 ppt/yr (p < 0.001)
23	162	4.6	2.2	2.3	1.5	3.0	= + 1.40 ppt/yr (p < 0.001)
24	105	0.9	3.0	0.8	0.7	1.0	NS

Table 3. pH: Mean, Median, Distribution Free 95% Confidence Interval, and Trend (Seasonal Kendall test).

Site	N	mean	skew	median	95% CI		trend
1	147	7.93	0.13	7.95	7.74	8.10	= + 0.072 (p < 0.001)
2	156	8.20	0.42	8.17	8.05	8.24	= + 0.047 (p < 0.001)
3	156	8.26	0.35	8.16	8.06	8.29	= + 0.095 (p < 0.001)
4	125	8.31	0.85	8.22	8.14	8.32	NS
5	105	8.38	0.38	8.26	8.11	8.48	NS
6	123	8.49	-0.13	8.58	8.34	8.69	= + 0.078 (p < 0.05)
7	159	8.11	0.82	8.05	8.00	8.12	= + 0.037 (p < 0.001)
8	62	8.64	0.80	8.57	8.45	8.69	NS
8.5	93	7.97	0.25	8.02	7.81	8.18	= + 0.120 (p < 0.01)
9	155	8.14	0.28	8.11	8.03	8.18	= + 0.047 (p < 0.001)
10	156	8.09	-0.07	8.04	7.98	8.10	= + 0.043 (p < 0.001)
11	164	8.58	-0.01	8.60	8.49	8.71	= + 0.090 (p < 0.001)
12	166	8.28	0.51	8.24	8.17	8.32	= + 0.033 (p < 0.001)
13	149	8.56	0.17	8.56	8.51	8.64	= + 0.087 (p < 0.001)
14	170	8.27	0.46	8.20	8.16	8.27	= + 0.023 (p < 0.05)
15	183	8.20	1.15	8.13	8.10	8.17	= + 0.031 (p < 0.001)
16	142	8.25	0.77	8.18	8.10	8.24	NS
17	141	8.40	0.46	8.39	8.21	8.49	NS
18	170	8.65	-0.10	8.64	8.56	8.75	NS
19	159	8.24	2.63	8.22	8.14	8.30	= + 0.031 (p < 0.05)
20	157	8.46	0.02	8.43	8.37	8.53	NS
21	132	8.42	0.09	8.40	8.32	8.52	NS
22	98	8.69	0.12	8.65	8.57	8.82	= + 0.100 (p < 0.001)
23	157	8.62	-0.03	8.64	8.53	8.73	NS
24	102	8.42	0.19	8.41	8.34	8.51	NS

Table 4.Dissolved Oxygen: Mean, Median, Distribution Free 95% Confidence Interval, and Trend (Seasonal Kendall test).

Site	N	Mean	Skewness	Median	95% CI		Trend
1	143	8.95	1.07	8.66	7.43	9.26	NS
2	146	8.19	0.97	8.22	7.8	8.75	+ 0.26 mg L^{-1} yr^{-1} ($p < 0.001$)
3	142	8.79	1.43	8.01	7.45	9	+ 0.38 mg L^{-1} yr^{-1} ($p < 0.001$)
4	116	9.18	0.52	8.89	8.52	9.67	NS
5	96	8.71	0.55	8.69	8.1	9.6	NS
6	108	9.60	0.62	9.19	8.1	10.22	+ 0.62 mg L^{-1} yr^{-1} ($p < 0.01$)
7	160	7.80	0.71	7.70	7.3	8.23	+ 0.1 mg L^{-1} yr^{-1} ($p < 0.05$)
8	59	9.35	-0.01	9.62	7.98	10.63	NS
8.5	83	7.40	0.42	7.20	6.3	8.3	NS
9	151	8.04	0.82	7.86	7.5	8.22	+ 0.20 mg L^{-1} yr^{-1} ($p < 0.001$)
10	155	7.74	0.75	7.59	7.15	7.91	+ 0.12 mg L^{-1} yr^{-1} ($p < 0.01$)
11	152	8.15	0.35	7.91	6.9	9	+ 0.29 mg L^{-1} yr^{-1} ($p < 0.05$)
12	152	9.08	0.86	9.05	8.35	9.4	+ 0.26 mg L^{-1} yr^{-1} ($p < 0.01$)
13	141	9.05	0.60	8.53	8.11	9.35	+ 0.37 mg L^{-1} yr^{-1} ($p < 0.01$)
14	162	8.73	0.37	8.80	8.4	9.3	+ 0.15 mg L^{-1} yr^{-1} ($p < 0.01$)
15	174	8.81	1.26	8.75	8.4	9.13	+ 0.16 mg L^{-1} yr^{-1} ($p < 0.01$)
16	138	8.31	1.34	8.40	8	8.74	+ 0.12 mg L^{-1} yr^{-1} ($p < 0.05$)
17	135	8.95	0.41	8.50	7.9	9.55	+ 0.19 mg L^{-1} yr^{-1} ($p < 0.05$)
18	158	9.91	0.04	9.67	8.8	10.4	NS
19	157	8.96	1.30	8.80	8.15	9.21	NS
20	151	10.30	1.24	9.81	9.4	10.32	NS
21	127	9.07	1.02	8.80	8	9.12	NS
22	91	10.54	0.75	9.70	9.2	10.46	+ 0.91 mg L^{-1} yr^{-1} ($p < 0.001$)
23	138	11.76	0.74	10.80	10.1	11.8	NS
24	94	10.70	1.09	9.90	9.61	10.69	NS

Table 5. Turbidity: Mean, Median, Distribution Free 95% Confidence Interval, and Trend (Seasonal Kendall test).

Site	N	mean	skew	median	95% CI		trend
1	115	40.69	3.67	23	17.8	34.4	+ 9.2 NTUs yr-1 (p<0001)
2	120	22.48	2.64	13.65	10	18.7	+ 6.0 NTUs yr-1 (p<0001)
3	121	23.69	3.49	9.5	7	11	+ 6.4 NTUs yr-1 (p<0001)
4	92	8.58	3.55	5.25	3.5	6.1	+ 4.0 NTUs yr-1 (p<0001)
5	82	63.24	4.10	27.35	15.8	45	+ 39 NTUs yr-1 (p<0001)
6	92	78.86	5.87	33.85	23	55.4	+ 35 NTUs yr-1 (p<0001)
7	124	9.82	2.33	7	5.5	8	+ 2.2 NTUs yr-1 (p<0001)
8	30	28.99	0.92	16.6	9.7	42.5	N/A
8.5	93	33.78	4.16	9.3	20	13	+ 2.3 NTUs yr-1 (p<0001)
9	123	7.16	3.15	5	4.5	6	+ 1.3 NTUs yr-1 (p<0001)
10	123	10.94	4.04	6.5	5.5	8	+ 2.3 NTUs yr-1 (p<0001)
11	134	35.94	3.28	19.15	15	25	+ 9.5 NTUs yr-1 (p<0001)
12	134	21.34	2.03	9.75	6.3	14	+ 4.8 NTUs yr-1 (p<0001)
13	120	18.10	1.74	9.25	7.3	12	+ 6.9 NTUs yr-1 (p<0001)
14	137	13.16	1.92	8	5.5	10.4	+ 3.3 NTUs yr-1 (p<0001)
15	143	12.13	2.85	4.7	3.5	6.7	+ 9.2 NTUs yr-1 (p<0001)
16	107	14.30	2.28	5.8	4.5	9.3	+ 3.0 NTUs yr-1 (p<0001)
17	111	22.67	1.86	8.8	6.5	13	+ 6.7 NTUs yr-1 (p<0001)
18	139	17.86	2.27	6.5	4.8	8.2	+ 3.3 NTUs yr-1 (p<0001)
19	126	44.65	3.62	23	15	36.7	+ 11 NTUs yr-1 (p<0001)
20	125	60.17	4.34	34	25.3	41.8	+ 15 NTUs yr-1 (p<0001)
21	101	100.02	3.91	62.6	52	79.6	+ 28 NTUs yr-1 (p<0001)
22	99	52.10	5.96	24	15.1	32	+ 5.7 NTUs yr-1 (p<001)
23	124	46.07	4.92	24.5	18	35	+ 32 NTUs yr-1 (p<0001)
24	68	68.45	0.12	73.2	54.2	24.5	+ 31 NTUs yr-1 (p<0001)

Nutrient concentrations in the slough varied dramatically in the slough. Nitrate concentrations ranged from <0.5 to 6420 mM. Median nitrate concentrations at each location ranged from 5.1 to 1258 µM (Table 6). Nitrate concentrations were low near the mouth but high concentrations were observed in the north end and south extremes of the sampling locations. The highest concentrations occurred in the southern portion of the slough (Tembladero Slough, Salinas River Bridge, Salinas River Lagoon, South Potrero Rd, and Monterey Dunes Way). In the northern portion of the slough, median nitrate concentrations were elevated but not as high as the south. However, the maximum nitrate concentration was found at Hudson's Landing East.

Generally, median ammonium concentrations for each site were highly variable within sites, and median concentrations ranged from 3.46 to 30.71 µM (Table 7). The highest concentrations occurred in the Strawberry Road site for sampling initiated in April 1998. Azevedo ponds had some of the highest ammonium concentrations observed. We also noted high ammonium concentrations in the Reserve, North Marsh and Tembladero Slough.

Median ortho-phosphorous concentrations for each site ranged form 1.6 to 21.9 µM (Table 8), High ortho-phosphorous concentrations generally occurred in the northern and southern parts of the slough and in Bennett Slough. Many sites were prone to spikes of high ortho-phosphorous concentrations, even in the main channel of the slough (e.g. Kirby Park). The highest median concentrations occurred in Tembladero Slough and the Lower Azevedo Pond.

Description of Seasonal Water Quality Patterns

Many of the water quality parameters related to seasonality, and there were some universal patterns across all the sampling locations. Using a one-way nonparametric test for quarterly time segments, we found a strong seasonal pattern in most of the parameters in many locations, over 50% of the sites had $p < 0.05$ (data not shown); however, the patterns were not the same for all the locations. In general, temperature spiked in the summer months and bottomed in the winter months. The seasonality was significant at all the sites monitored. Salinity also dropped in the winter months in all locations except in the Old Salinas River, Salinas River Lagoon, and Salinas River, with median concentrations below six parts per thousand (ppt) all year around. Limited evidence existed for seasonality in turbidity measurements, although a few sites had higher NTUs in the winter and spring months. Twelve sites had significantly different dissolved oxygen concentrations; most of them had the lowest concentrations in the summer months. The lower dissolved oxygen concentrations usually occurred in the main channel and the channel north and south of the marsh. Areas in the northern portion of the slough did not have seasonal patterns in dissolved oxygen concentrations. Twelve sites had seasonal differences in pH where pH was generally highest in the last spring and summer months. These patterns occurred throughout the slough at various locations without a spatial pattern.

Nutrient concentration exhibited strong seasonal trends, but these trends varied by area of the slough. The two main freshwater source of water had variable nutrient concentrations. Carneros Creek has relatively high ammonium and ortho-P concentrations compared to the Salinas River. However, spikes of high concentrations occurred regularly with ammonium, while ortho-P patterns were more seasonally driven. Nitrate concentrations were higher in the Salinas River especially before 1995. Nitrate concentrations declined for brief periods during the rainy season.

In the north end of the slough, the lowest nitrate concentrations occurred in the late summer and fall. Concentrations were significantly higher in the winter months. However, in the southern sites, concentrations were highest in the summer, while in the fall concentrations were generally lower. Summer nitrate concentrations, however, remained the highest of the sampling locations. In contrast, 14 sites had significant seasonal difference in ammonium concentrations, and nearly every site had the highest concentrations in the winter. Even the sites not statistically significant seasonally, generally had the highest median concentrations during the winter months. Four sites did not have a seasonal pattern for ortho-P. There were strong differences in how these seasonal differences occurred geographically. The highest ortho-P concentrations occurred during the summer months in the upper part of the slough to Kirby Park. The Azevedo Ponds, however, showed highest concentrations in the fall. The channel north of the mouth had its highest ortho-P concentrations in the spring, and the southern portion of the slough had the highest median concentrations in the winter months.

Non-parametric Evidence for Long-term Trends

Using the Seasonal Kendall analysis to calculate the relationship between water quality and sampling date, we found many significant results (Tables 1-8). Thirteen of the 25 locations had a significant increase in temperature over the sampling period. The increasing temperatures ranged from 0.09 to 0.45^{o}C/year. Scattered throughout the slough the increase in temperature did not reflect an obvious spatial pattern. The trend in salinity also varied across the slough (Table 2). Several sites in the northern part of the slough and southern portion of the slough declined significantly in salinity, while several sites in the central part of the slough had an increase in salinity. Of the 25 sites, 15 sites had a significant increase in pH units over the sampling period (Table 3). The highest increase occurred at the Salinas River Lagoon (0.1 pH units/year). In general, the areas in the southern part of the slough, where freshwater flow is considerable, had the fewest significant trends. Turbidity and dissolved oxygen appear highly variable during through the monitoring period. In 14 of the sites, dissolved oxygen concentrations increased between 0.1 and 0.9 mg/L/year (Table 4). The largest increase occurred in the Salinas River Lagoon, which had low concentrations at the beginning of the monitoring. The median turbidity for each site ranged from 1.3 to 39 NTUs/year (Table 5). The trend analysis did not include Strawberry Road because of a limited number of observations. The sites with the highest turbidity increases included Azevedo Ponds (Central and South), Old Salinas River at Monterey Dunes Way, Salinas River at Highway 1 and Tembladero Slough.

The trends in nutrient concentrations were highly variable. Nine sites had a significant increase in nitrate concentration ranging from 1.2 to 96.6 μM/year (Table 6). However, two sites had a decline in nitrate concentration. The sites of Strawberry Road and Salinas River at Monterey Dunes Way had a significant decline in nitrate concentrations. Ammonium concentrations increased nine sites between 0.5 and 1.5 μM/year (Table 7). The North Marsh site declined in ammonium over its sampling period before removal from the sampling route in 1998. Seven locations had significant increases in ortho-Phosphorus (P) with concentrations ranging from 0.11 to .64 μM/year (Table 8). These increases generally occurred at the north end and in the Salinas River and the Salinas River Lagoon. Four locations had a decline in ortho-P including one of the Azevedo Marshes (South Pond) and Struve Pond/Slough north of the mouth of the main channel. These declines ranged from 1.0 to 0.45 μM/year.

Table 6. Nitrate: Mean, Median, Distribution Free 95% Confidence Interval, and Trend (Seasonal Kendall test)

Site	N	mean	skew	median	95% CI		trend
1	147	109.0	3.2	48.4	32.2	64.5	NS
2	158	156.2	5.4	48.4	32.2	28.7	+ 6.2 uM/yr (p < 0.001)
3	161	266.3	6.1	54.8	32.2	80.6	+ 5.8 uM/yr (p <0.01)
4	121	52.3	3.6	32.3	16.1	32.2	NS
5	109	53.0	4.7	16.1	8.1	32.2	NS
6	123	75.8	7.6	16.1	8.1	32.2	NS
7	154	35.0	5.7	16.1	8.1	16.3	+ 1.2 uM/yr (p < 0.05)
8	61	118.9	3.2	32.3	16.1	80.6	- 23.2 uM/yr (p < 0.05)
8.5	94	27.8	2.8	5.1	2.6	16.1	NS
9	146	27.1	3.0	16.1	8.1	16.1	+ 2.4 uM/yr (p < 0.01)
10	154	39.8	6.1	16.1	16.1	32.2	+ 1.2 uM/yr (p < 0.01)
11	151	57.9	5.3	16.1	8.1	32.2	+ 1.2 uM/yr (p < 0.05)
12	139	35.4	2.6	16.1	8.1	16.1	NS
13	134	30.1	3.3	11.3	8.1	16.1	NS
14	154	42.9	3.0	16.1	8.1	32.2	NS
15	156	97.5	4.2	32.3	16.1	32.2	NS
16	149	206.3	7.3	112.9	80.6	129.0	NS
17	141	85.6	3.3	48.4	32.2	64.5	NS
18	157	126.7	3.4	32.3	32.2	48.4	+ 2.8 uM/yr (p < 0.05)
19	165	606.6	1.5	388.8	290.0	548.0	+ 16.1 uM/yr (p < 0.01)
20	166	1157.8	1.0	963.9	888.0	1096.0	NS
21	141	1251.1	1.0	1080.6	983.0	1225.0	- 60.6 uM/yr (p< 0.001)
22	101	899.9	1.5	677.4	677.0	871.0	+ 96.6 uM/yr (p < 0.001)
23	164	1071.2	1.3	857.9	774.0	975.0	NS
24	111	1391.2	1.3	1258.1	1064.0	1516.0	NS

Table 7. Ammonium: Mean, Median, Distribution Free 95% Confidence Interval, and Trend (Seasonal Kendall test).

Site	N	mean	skew	median	95% CI		trend
1	149	26.49	3.49	14.29	11.43	17.50	+ 1.1 uM yr-1 (p < 0.05)
2	158	11.69	1.63	8.46	7.14	9.29	NS
3	156	16.29	5.19	7.86	6.43	10.00	NS
4	126	9.85	1.71	7.14	6.43	10.00	NS
5	111	25.70	6.82	9.29	5.71	12.86	NS
6	122	18.31	8.17	7.14	5.71	9.29	NS
7	159	8.00	1.83	6.43	5.71	7.14	NS
8	61	19.27	2.76	9.29	5.71	12.14	-0.9uM yr^{-1} (p < 0.05)
8.5	94	37.00	3.89	20.71	14.29	27.14	NS
9	155	6.22	1.58	5.53	4.29	6.43	+ 0.3 uM yr-1 (p < 0.001)
10	159	8.69	4.70	7.14	7.14	8.46	+ 0.25 uM yr-1 (p < 0.05)
11	152	21.61	5.39	7.14	5.71	9.29	+ 0.6 uM yr-1 (p < 0.01)
12	150	8.73	7.41	6.43	5.71	7.14	NS
13	134	10.70	6.30	4.64	3.57	5.89	NS
14	156	6.83	3.07	5.00	4.29	5.71	NS
15	162	8.12	2.07	6.43	5.00	7.14	NS
16	145	10.90	3.07	7.14	6.43	7.86	NS
17	145	22.02	3.40	9.29	7.86	10.71	+ 0.5 uM yr-1 (p < 0.05)
18	159	19.26	3.80	7.14	5.71	8.57	+ 0.3 uM yr-1 (p < 0.05)
19	159	13.39	2.98	10.00	8.57	12.14	+ 0.5 uM yr-1 (p < 0.01)
20	158	16.00	2.80	9.81	7.86	12.14	NS
21	134	17.54	2.27	12.14	10.00	13.57	NS
22	102	8.53	3.23	3.46	1.95	5.71	+ 1.5 uM yr-1 (p < 0.001)
23	153	12.09	7.91	5.62	4.29	6.43	+ 0.5 uM yr-1 (p < 0.001)
24	109	83.60	10.41	15.71	12.14	20.00	NS

Table 8. Ortho P: Mean, Median, Distribution Free 95% Confidence Interval, and Trend (Seasonal Kendall test).

Site	N	mean	skew	median	95% CI		trend
1	153	16.35	2.90	6.13	4.84	8.71	+ 0.339 uM/year (< 0.05)
2	157	6.10	4.10	4.52	4.19	5.48	+ 0.191 uM/year (< 0.01)
3	161	10.87	2.58	7.10	5.81	8.71	+ 0.527 uM/year (< 0.001
4	132	3.40	2.15	2.58	2.26	3.23	NS
5	108	8.24	1.94	4.84	3.55	5.81	NS
6	131	24.49	2.05	17.74	16.13	20.65	- 1.04 uM/year (< 0.05)
7	163	3.80	5.24	3.10	2.58	3.23	NS
8	59	3.16	2.41	1.94	1.29	2.58	NS
8.5	91	3.17	3.34	1.61	1.29	2.90	NS
9	158	4.05	5.48	2.58	2.26	2.60	+ 0.108 uM/year (< 0.01)
10	159	4.10	2.72	2.58	2.26	3.23	NS
11	157	16.47	2.10	10.97	9.35	14.78	- 0.1.51 uM/year (< 0.001
12	154	7.10	4.02	4.84	3.87	5.48	NS
13	139	8.33	10.48	4.84	3.87	5.48	- 0.452 uM/year (< 0.001)
14	161	5.06	2.34	3.23	2.90	3.87	- 0.108 uM/year (< 0.05)
15	161	4.19	2.48	2.58	2.26	2.90	+ 0.108 uM/year (< 0.05)
16	147	6.34	2.44	3.87	3.23	4.84	NS
17	143	11.10	3.89	3.87	3.23	5.48	+ 0.242 uM/year (< 0.01)
18	161	11.75	3.88	5.16	4.19	6.77	NS
19	162	11.32	2.17	8.49	6.45	10.32	NS
20	164	14.50	0.99	13.71	12.58	15.81	NS
21	139	13.45	0.86	10.65	9.03	13.23	NS
22	99	4.67	7.10	3.23	2.58	4.19	+ 0.645 uM/year (< 0.01)
23	157	4.49	7.91	3.55	2.90	4.19	+ 0.211 uM/year (< 0.01)
24	111	22.18	0.67	21.94	20.00	23.55	NS

Comparing water quality at three locations

Porter Marsh has a history of relatively high salinity concentrations; however the concentrations show a decline during the rainy season. Over time, an increase nitrate variability and concentration except for 2004 and 2005 suggest that upstream land use changes resulted in wate quality improvements Except for the last two-three years, nutrient concentrations appear have increased with time. Kirby Park salinity is slightly less than the ocean, except for wide discursions to lower values during rainfall events. Varying Nitrate concentrations appear to be increasing, while there is no obvious pattern for ammonium and ortho-P. The water quality in Azevedo Pond show highly variable salinities and range from near seawater concentrations to nearly fresh to hypersaline. Nitrate and ortho-P have years with relatively high concentrations and low concentrations and no obvious correspondence between them. Ammonium was relatively high until 1998 and has declined and remained relatively low since 1998.

Data Preparation for Time Series Analysis

Data collected nominally on a monthly basis do have some observations missing. However, a few months have two samples taken. When a month with no samples followed or preceded a month with two samples, sample dates were often close to the extreme days of the month. In those cases, we moved the sample closest to the empty month. Otherwise, we removed the sample with fewest measured variables. After this step to move or remove data, 22% monthly of the data were missing. Additionally, we corrected or removed anomalous results, e.g. obvious data entry errors. We handled the missing data by replacing the missing values with the median of the observations from the remaining years for the corresponding month.

General Approach to Time Series Analysis

We performed a number of data analyses to the data collected in the ESNERR between 1988 and 2004. We focused on the estimation of possible trends for each of the different water quality measurements. The estimation of global trends in the slough accounts for the following factors:

- Temporal correlation between observations: Temporal correlations affect the estimation of the variability needed to establish the significance of trends; under the presence of high temporal correlation, trend coefficient standard errors are underestimated. This underestimation increases the probability to reject the null hypothesis of no trend.
- Missing values: Missing values are present both casually and systematically for extended periods.
- Strong spatial variability: The slough has a complicated hydrology affecting local measurements. We found it difficult to establish associations based on proximity of sites. We did not find the existence of common global trends and, for each type of measurement, resorted to grouping the observations. As an example, for the water temperature we considered a mixture of two distributions one corresponding essentially to coastal stations and one to inland stations.
- Regular and representative sampling: Observations are taken usually at monthly intervals. Our analyses assume that such observations are representative of the conditions during the month. This clearly involves a representativeness error impossible to estimate with only one observation per month per location.
- Observational errors: Observational errors can be included, but factors other than the instrument precision, as reported by the manufacturer, are difficult to assess, as there are no replicate data.

Below we list some of the steps found to be relevant for the data analysis:

1. Data alignment: When a month with no samples followed or preceded a month with two samples, these were often close to the extreme days of the month. In those cases, we moved the sample closest to the empty month.
2. Stations indexing: We indexed the stations with respect to their distance to the mouth of the slough.
3. We performed an exploratory data analysis consisting mainly of: (a) comparing the distributions for each month; (b) comparing the distribution for each location;

(c) calculating linear trends, after removing seasonal components, for each location, and plotting the coefficients as a function of the distance to the mouth.

4. We explored the residuals of such as simple fit, for each location, to determine serial and spatial correlations.
5. We used seasonal Kendal tests to obtain a preliminary assessment of the significance of the trends in each series.
6. We fitted models for transformations, seasonal trends, long-term linear trends and serial correlations. We accounted for missing values within the estimation procedure.
7. We explored the goodness of fit of such models explained above.
8. We compared and summarized the results from all stations.

These are general steps. Each water quality variable has peculiarities. These peculiarities required careful modeling and specific estimation techniques.

Results and Conclusions

Spatial and Seasonal Patterns

Water quality in Elkhorn Slough had remarkable spatial variation with concentrations ranging across five orders of magnitude for nitrate and ammonium and four orders for ortho-P. These lowest concentrations occurred in the main channel or areas of the Estuarine Reserve where there is a great deal of tidal flushing or adjacent upland areas managed as natural habitat. Areas of the highest nutrient concentrations had limited tidal flushing and adjacent land uses dominated by agriculture or have upstream municipalities (Salinas River). For example, we found the highest median nutrient concentrations at Moro Cojo Slough along the Salinas River (Bridge, Monterey Dunes Way, Potrero Road, and Lagoon) and Azevedo Ponds. Historically, these waterways functioned a complex of fresh, brackish, and salt water habitats, however, currently they function as agricultural drainage ditches with limited habitat value. The northern portions of slough also had elevated nutrient concentrations, but varied dramatically based on fresh water inflows

Turbidity Changes

Turbidity has increased throughout the slough, but the cause is uncertain. Water column turbidity changes may be due to increasing phytoplankton biomass and/or suspended sediments implies the reduction decreases eelgrass habitat. We suggest a better understanding of algae production and a focused study on suspended sediment in the slough. This would include particle size distributions, organic matter content, and some attempt of source tracking. It is particularly important to understand the relative role of tidal scour, terrestrial erosion sources, harbor activity, and water column generated processes (microbial production and decomposition).

Turbidity in the in the upper slough, harbor areas, north mouth areas, and the Salinas-Tembladero complex were greatest in the winter months (usually February and March). These months correspond to times of consistent freshwater flow into the slough. In contrast, the central marshes have maximum turbidity measures in the early spring to summer months. This turbidity may correspond to phytoplankton activity. Turbidity in the Azevedo Ponds were variable and may reflect a combination of phytoplankton growth, wind driven bottom sediment turbidity and erosional processes from surrounding farming activity and runoff.

Time Series analysis of Temperature

Authors

Ricardo T. Lemos, Maretec—Instituto Superior Técnico, Universidade Tecnica de Lisboa, Portugal rtl@net.sapo.pt.

Marc Los Huertos, Science and Environmental Policy, California State University, Monterey Bay, 100 Campus Center Drive, Seaside, CA 93955.

Bruno Sanso, Applied Mathematics and Statistics, 1156 High Street, University of California, Santa Cruz, CA 95064.

Abstract

We expected temperature should be the most tractable of all the water quality measures. For example, nutrient concentrations tend to be highly variable, and dissolved oxygen or turbidity measures are controlled by several factors simultaneously (e.g., sediment concentration, planktonic and benthic algae, water mixing, nutrient concentrations, and day length). The results presented in this paper used increasingly complex statistical approaches. At the onset, visual inspection of the data strongly suggests temperatures and their seasonal amplitudes are increasing in the slough in most of the 24 sampled sites. In this paper, we carefully quantify such trends.

Introduction

Dating back to the 1880s, human changes to the slough's hydrology have strongly influenced water temperature. Because of the artificial opening of the main channel to create a harbor for fishing and research vessels, the slough experiences semi-diurnal tidal action. In the lower portion of the slough, water has a residence time of less than one day. In the northern portion of the main channel, water has a longer residence time, estimated to be 3 weeks (personal communication Steve Monosmith). Currently, the main channel extends inland for 11.4 km from Monterey Bay in Central California (Figure 2). The slough includes a variety of habitats. These slough habitats receive seawater exchange through the mouth and terrestrial freshwater from a few seasonal streams in upper Elkhorn main channel (Carneros and Corncob Canyon Creek), plus flow from Salinas River, via the Old Salinas Channel, and runoff from local terrestrial sources. Thus, some areas have limited tidal exchange isolating temperatures from the main channel, while other areas have extremely high tidal exchange and temperatures similar to the ocean. Augmented by agricultural run-off, flow in many of the freshwater sources often in the form of summer irrigation tailwater or winter storm driven events.

Exploratory Analysis

We expected, of all the water quality measures, temperature should be the most tractable. For example, nutrient concentrations tend to be highly variable, and dissolved oxygen or turbidity measures are controlled by several factors simultaneously (e.g., sediment concentration, planktonic and benthic algae, water mixing, nutrient concentrations, and day length). The results presented in this paper were obtained after using increasingly complex statistical approaches. At the onset, visual inspection of the data strongly suggests temperatures and their seasonal amplitudes are increasing in the slough in most of the 24 sampled sites. Based on these changes, we renumbered the locations to better display how temperature patterns depend on the distance from the mouth of the estuary (Figure 2). Note, the numbering in the rest of the report is based on Figure 1.

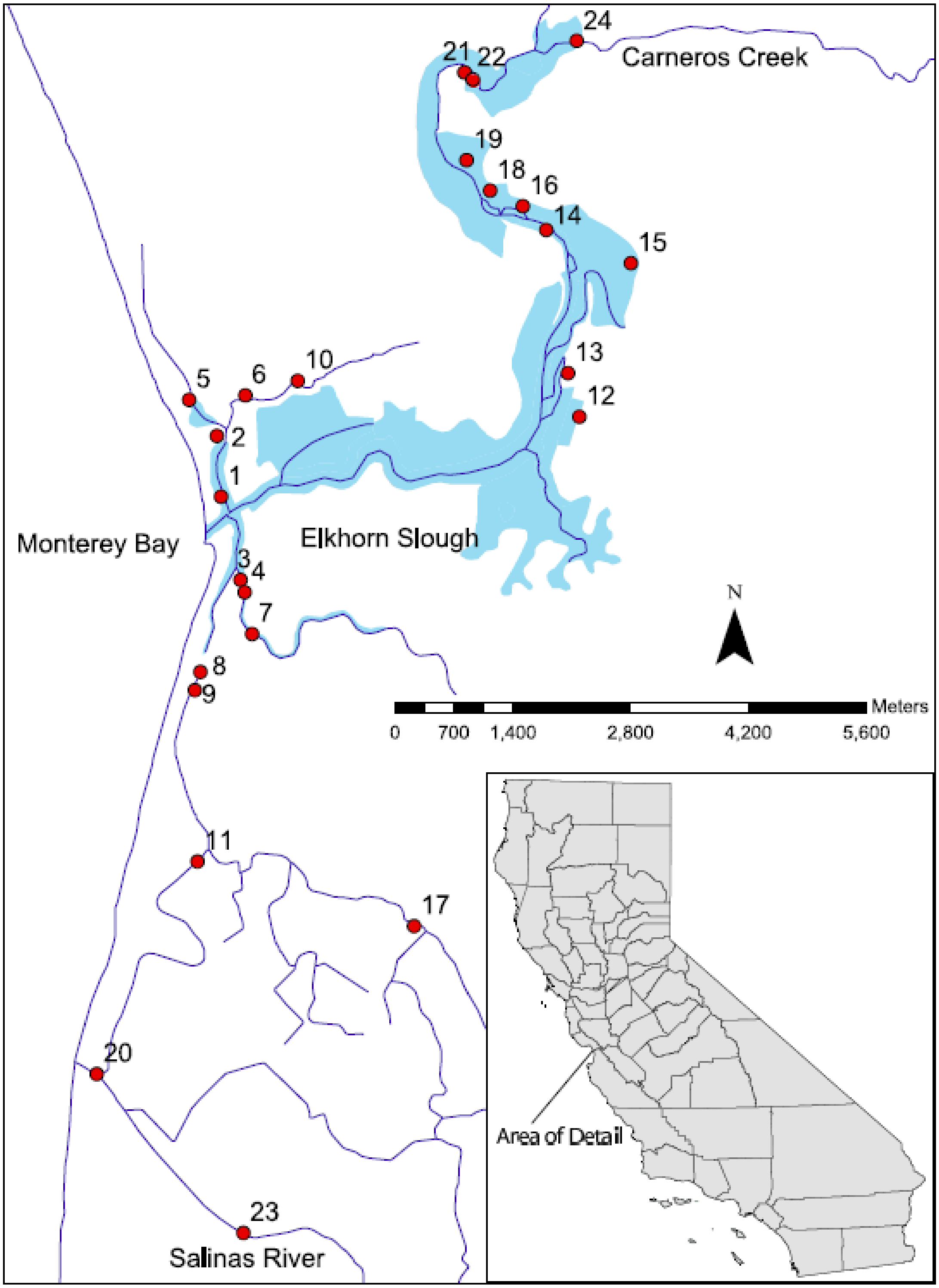

Figure 2. Sampling locations renumbered for this section.

Our exploratory data analysis began with time series plots of temperature at the 24 stations. Given the strong seasonal signal immediately apparent, we attempted to model each time series as the sum of a stationary seasonal cycle, with sinusoidal shape, a linear trend and random white noise. Preliminary results derived from these models revealed several important features in the data. First, the seasonal signal varied markedly from station to station in terms of amplitude, ranging between 4.5^{o}C and 12.5^{o}C. In contrast, the phase appeared locked, with the yearly minimum occurring in January. Secondly, 19 out the 24 stations presented long-term warming trends, up to 4^{o}C in 16 years. Despite being smaller than yearly amplitudes, the warming trends seemed evident upon visual inspection of fitted values together with observations. A seasonal Kendall test supported the significance of such trends. The tests consist of a non-parametric test well suited to data with strong seasonal patterns. In this case, we used month as the season (i.e. 12 seasons per year). Results suggested 13 of the 24 sites had a significant increase in temperature over the sampling period. The increasing temperatures range from 1.1 to 5.4^{o}C accross 16 years. Stations with significant trends appear scattered throughout the slough and do not reflect an obvious spatial pattern. In some stations, an amplification of the seasonal cycle, with warmer summer months, seem to be occurring, rather than a year-round temperature increase.

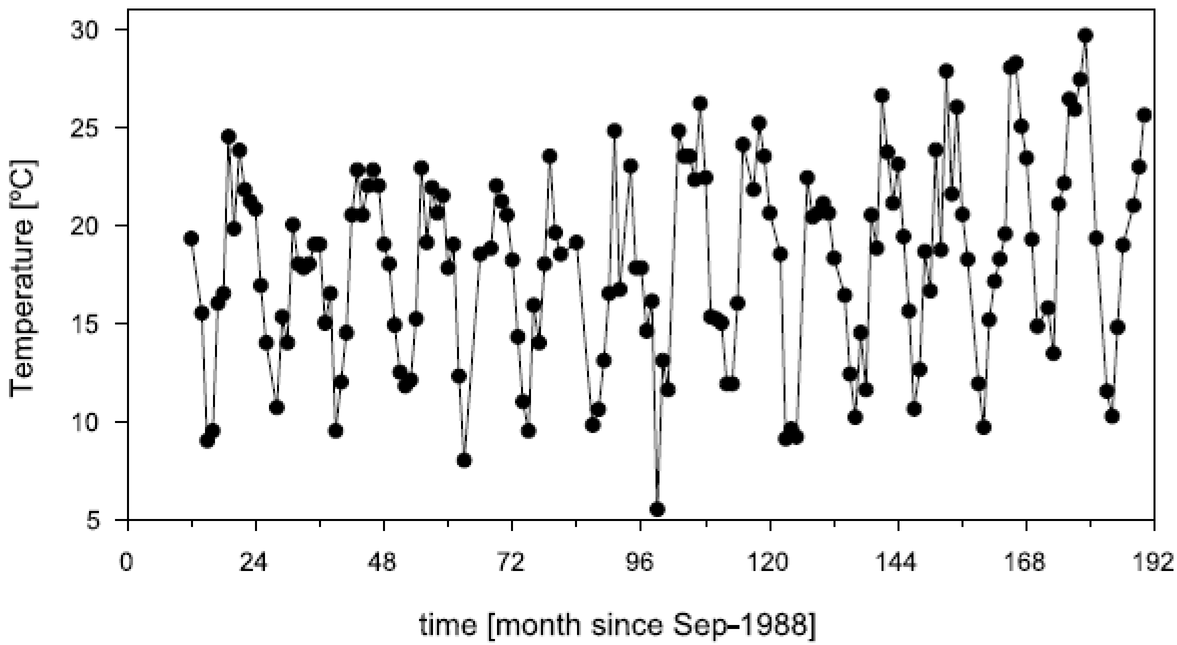

Figure 3. Time series data of temperature for Station 22.

In contrast to our initial expectations, both trends and seasonal cycles were not always similar for nearby stations. Even with factors, such as connectivity and tidal influence, we could not find simple methods based on proximity to appropriately estimate the results for a given station given the neighboring ones. This reflects the complex circulation patterns present in estuarine systems, and hinders the interpolation of observations to other locations in the estuary, as we first intended.

More importantly, the simple statistical models mentioned above could not adequately describe temperature variability in the Elkhorn Slough. The residual analysis revealed the presence of substantial unexplained structure. For instance, observations made in April systematically produced positive residuals, indicating one sinusoidal component was not enough to capture the annual cycle of temperature. As will be depicted below, this complex cycle required a form-free model separating the effects of each month. Conversely, we found significant spatial and temporal correlations in the residuals. This impaired any estimate of significance assigned to the trends, and implied the need for additional model parameters. Interestingly, the time series of residuals obtained with stationary form-free models with linear trends were similar among stations. This feature pointed to a common explanatory variable to the short-term variability of temperature in the slough. We considered solar radiation, rainfall and wind speed, measured in the weather station of Castroville, as well as sea surface temperature (SST) data from a National Oceanic and Atmospheric Administration (NOAA) buoy located off the Monterey Bay. From a visual inspection of time-series plots, we concluded a known combination of some of these variables – potential evapotranspiration -- might provide the best regression variable.

As we moved into models with form-free seasonal components, we observed coastal stations, clearly influence by the entrance of seawater into the slough, display a damped seasonal cycle of temperature variation similar to that of offshore SST. In contrast, temperature of inland stations behaved more like air temperature, cooling slightly more in winter and warming much more during summer. Thus, we hypothesized each station's cycle could be a mixture of two seasonal patterns. We could not deduce the exact mixture from the station's location; however, we greatly reduced the dimensionality of the problem.

The quantification of the temperature trends summarized the main results from our analysis. We show such trends vary substantially from month to month and from station to station. In most cases, the summer temperature has increased by up to 5^oC in 16 years, while we observed a comparable decrease in April in other stations. Establishing the cause of this increase was beyond the scope of this effort.

Monte Carlo Method and Statistical Model

We expressed temperature as the sum of the following: a seasonal component, a trend component, a baseline dependent on atmospheric factors and random white noise. To account for the spatial variability of the seasonal cycle and the trends, each of these components if the result of a locations-specific mixture of two patterns of temperature change from inland temperature cycles, and one from the two trend patterns to indicate warming. More explicitly the model for $\theta_{m,y}(s)$ (temperature of station (s), month (m) and year (y)) can be written as:

Equation 1

$$\theta_{m,y}(s) = \alpha(s)\eta_m^{(1)} + (1-\alpha(s))\eta_m^{(2)} + \beta(s)\gamma_m^{(1)}(t-\bar{t}) + (1-\beta(s))\gamma_m^{(2)}(t-\bar{t}) + \lambda_t + \varepsilon_{m,y}(s)$$

where t = t(y,m) = 12(y-y_1) + m, with y1=1988, and t = 95. For month m, $\eta^{(1)}_m$ and $\eta^{(2)}_m$ are the two temperature seasonal components, which we identify with the inland and coastal seasonal components, respectively. $\lambda^{(1)}_m$ and $\lambda^{(2)}_m$ are the two long-term linear trend components. For station, s, α(s)$ and β(s) correspond to weights (between zero and one) assigned to $\eta^{(1)}_m$ and $\lambda^{(1)}_m$, respectively. λ_t corresponds to the short-term temperature variability in the slough. The variability of λ_t has serial correlation and is partially explained using atmospheric factors, as will be seen below. Finally $\varepsilon_{(m,y)}(s)$ is random noise. For more information on model assumption, see Lemos, (in press).

The salient features of the model in Equation 1 include two different seasonal patterns described by twelve parameters each. This provides the flexibility needed to capture the lack of symmetry observed in the data, in particular, the dip observed from April to May at some stations. The hydrology of the slough suggests that monthly trends vary with geographical location. *A priori*, we have no reason to believe either coastal or inland stations display stronger long-term trends, because we do not know the cause for such temperature change. Therefore, we use different sets of weights for the seasonal signal (α) and the trends (β). In both cases, the model does not impose any spatial regularity; in fact, all our earlier attempts at considering seasonal patterns or trends linked by proximity were unsuccessful. Nor does the model impose any relation between the parameters that change with the month, since this would smooth out the peculiar effect of months like April and December.

We denote the observations taken at station (s), month (m) and year (y) as $x_{m,y}(s)$. We assume:

Equation 2

$$x_{m,y}(s) = \theta_{m,y}(s) + \chi_{m,y}(s), \chi_{m,y}(s) \sim N(0, \tau_\chi^2)$$

In words, the temperature at a given time and location is subject to a measurement error, $\chi_{m,y}(s)$. We assume that such errors are all independent across time and location.

Local weather stations (California Irrigation Management Information System -- CIMIS) continuously measure temperature, solar radiation, rainfall, relative humidity, and wind speed and direction and calculate reference evapotranspiration using the Penman-Monteith equation. The resulting output provides daily assessments potentially associated to drivers of short-term temperature trends in the slough. We complete the model specified by Equations 1 and 2 by incorporating reference evapotranspiration (ET_o), denoted as z_t, as an explanatory variable for λ_t. We chose such a simple seasonal model for ETo after a preliminary regression analysis suggested no additional sinusoids are needed. For more detail on how ET_o was incorporated into the model see Lemos, et al. (in press).

We assume all parameters have independent priors. We use sea surface temperatures from the National Oceanic and Atmospheric Administration buoy 46042, and air temperature data from CIMIS station 19, Castroville, to provide proper normal priors for the coastal and inland average monthly temperatures, respectively. For the trends, δ_1, κ_1, and φ, we assign vague normal priors, with mean zero. For more detail regarding the selection of priors and model fitting, MCMC procedures, and checking, refer to Lemos et al. (in press).

Results

Figure 4 shows the 95% posterior intervals corresponding to the two types of seasonality and trends. We observe both types of seasonality presented dip in May. This is consistent with the behavior observed in the data, where a strong decrease in temperature in May is present for most stations. $\eta^{(1)}$ is typical of inland stations, with higher temperatures, especially during the summer. For most months, the main effects of the two types of seasonality have little overlap. The long-term trends show substantial overlaps during the fall and winter months. Of particular interest, is the components of

$\gamma^{(1)}$ are mostly positive, while those of $\gamma^{(2)}$ are mostly negative. The monthly differences indicate, where present, the warming trend is not consistent through the year. In general, we observe the trend is stronger for summer months than for the rest of the year and there may be a cooling trend in April. We notice variations through the year for all of the stations. For the majority of the stations there is some evidence of warming, especially during the summer months. April is peculiar, since for some stations there is some evidence of cooling trend during that month. The stations where this effect is strongest are 2, 7, 9, 11, 14, 17 and 24. A strong warming trend is present in December for almost all stations. In some cases the warming can be as high as high as 5^{o}C/(16 years) in median, but its value is highly variable.

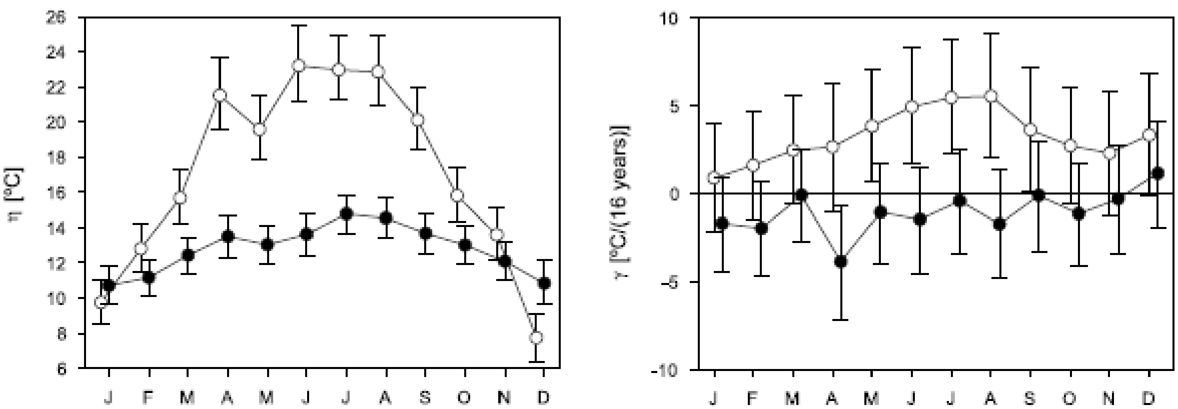

Figure 4. Posterior mean and 95% probability intervals for the parameters that define seasonality patterns (left panel) and trends (right panel). The open symbols correspond to $n^{(1)}$ and $y^{(1)}$, and the filled symbols correspond to $n^{(2)}$ and $y^{(2)}$.

The proportion of each type (i.e. coastal or inland) of seasonality or seasonal trend correspond to a station is shown in Figure 5. Since the stations, ordered with respect to their distance to the mouth, we expect some association between the x-axis in the plots and the weights. In fact, α(s) generally increases with increasing distance inland. This is particularly evident for the first seven stations. However, there is a great deal of variability due to local conditions. The behavior of the weights for the monthly seasonal trends is more irregular. Tidal stations and stations close to the coast (rank 14 with restricted flow due to structures in the channel, like tidal gates, culverts, etc. (muted), admit an even mixing of the two seasonal trend components. In contrast, most northern stations display average weights above 0.5. Station 24 is a clear exception.

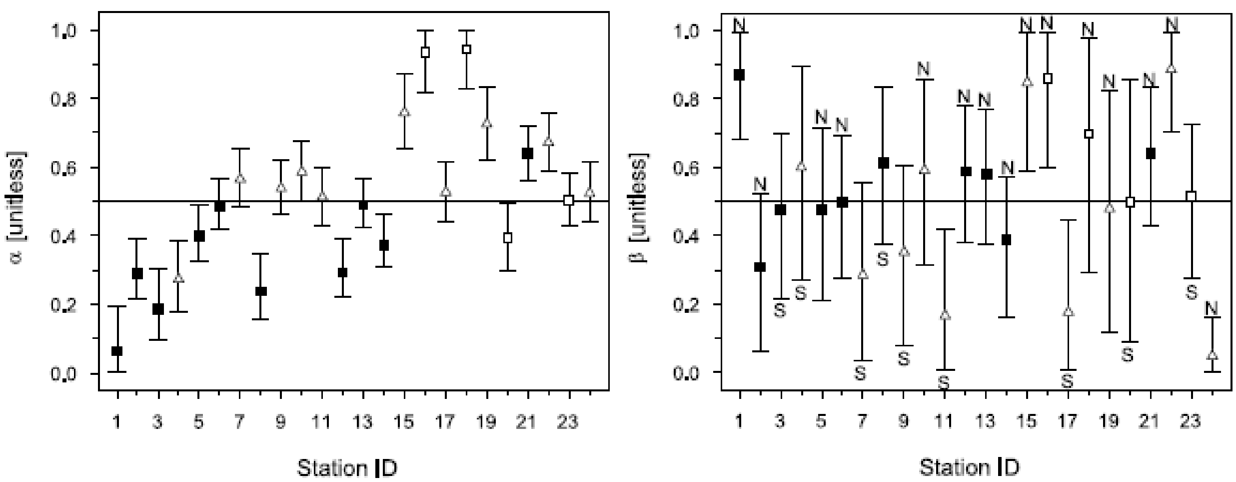

Figure 5. Posterior mean and 95% probability intervals for the weights α (left panel) and β (right panel). Filled squares correspond to tidal stations and open triangles to muted stations, and white squares to non-tidal stations. The horizontal lines provide the reference of even mixing of the two patterns. On the right panel, stations labeled with ‘N’ are located north of the mouth, those labeled with ‘S’ are located south of the mouth.

Figure 6 and 7 show the trend result for each station tests. We notice variations throughout the year for all of the stations. From the majority of the station there is some evidence of warming, especially during the summer months. April is peculiar, since for some stations there is some evidence of cooling trend ruing that month. The stations where this effect is strongest are 2, 7, 9, 11, 14, 17, and 24.

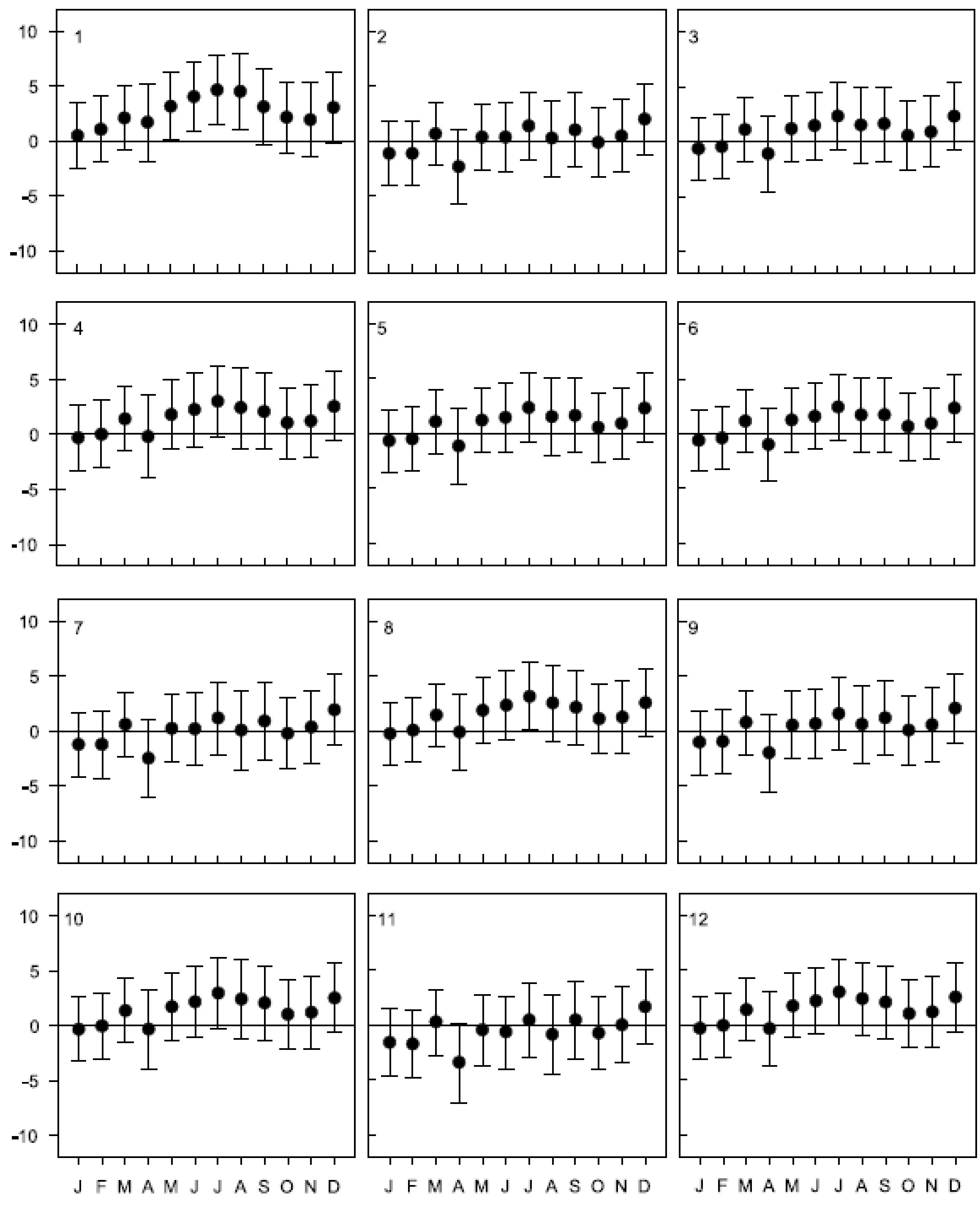

Figure 6. Posterior mean and 95% probability intervals for temperature trends estimated for Stations 1 to 12. The y-axis scale corresponds to ^{o}C/(16 years), representing the difference in temperature between 2004 and 1998.

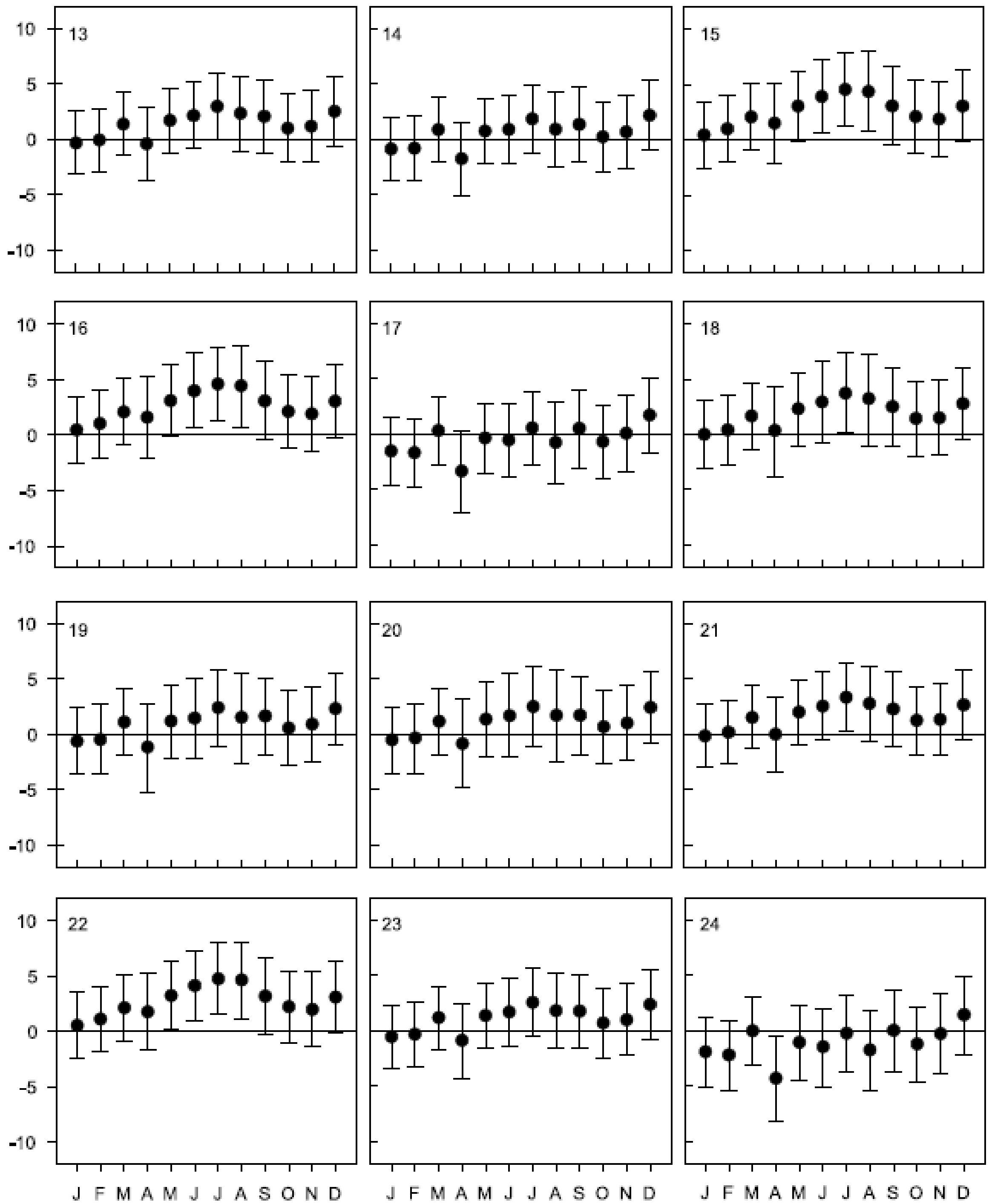

Figure 7. Posterior mean and 95% probability intervals for temperature trends estimated for Stations 13 to 24. The y-axis scale corresponds to ^{o}C/(16 years), representing the difference in temperature between 2004 and 1998.

Figure 8 shows an example of how the seasonal pattern changes with time. Station 22 has substantial changes for each moth, but the stronger differences are present during the summer months. The mean of the seasonal component has had an increase of about 4^{o}C.

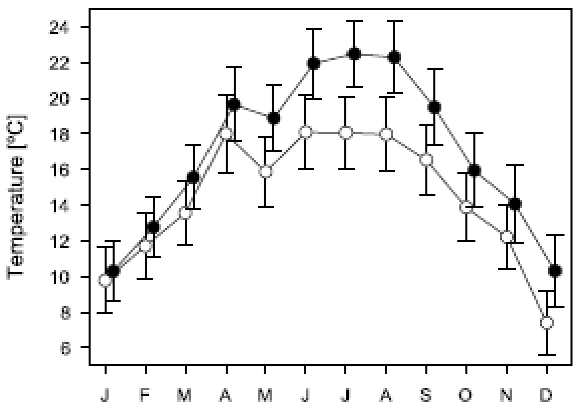

Figure 8. Posterior mean and 95% probability intervals for the seasonal cycle in the first year (open circles) and last year (close circles) for the time-series for Stations 22.

Discussion and Conclusions

Models considering time varying parameters have been successfully applied in a number of examples (Shaddick and Wakefield 2002; Huerta, et al. 2004, Lemos and Sansó 2006). The approach taken in Lemos and Sanso (2006) considers temperature trends varying smoothly in space. The model in Huerta et al. (2004) focuses on the spatial variation of the amplitudes of the series. Those approaches are not appropriate for the problem considered in this paper, since the complex hydrology of the slough produces localized effects. However, by using the free-form model and observations from a 16 year period, we successfully analyzed the spatial and temporal variations in temperature in Elkhorn Slough. The base assumption in the model assumed the within-year dynamics needed to display a mixture of two form-free patterns. Monthly variation of temperature, characterized by period of strong temperature change, contrasted with others of relative constancy, and a lack of symmetry. The patterns could be captured using sinusoidal components; however, the model would require as many parameters as the free-form representations. Given the results, we identify two free-form patterns: a coastal and inland pattern.

The monthly variation of temperature is clear and only three months separate the coldest and the warmest months of the year, i.e. December and April respectively. Periods of strong temperature fluctuations contrast with other months of relative constancy or steady variation. Sinusoidal components also captured this behavior; nevertheless, the lack of symmetry would require many terms, involving nearly as many parameters as the form-free representation. Given the results, we can broadly identify the two form-free components describing the coastal and the inland variation of temperature. The coastal component, when compared to its counterpart, has smaller annual amplitude and fluctuations. This is likely an effect from the buffering action of the ocean, since in this region the annual SST amplitude is smaller than $5^{o}C$. The maximum and minimum annual slough temperatures do not reflect either SST or air temperature. Thus, the slough temperatures may parallel regional extremes in the balance between radiation absorption and emission. Apart from tidal influence, site-specific effects seem to come into play, since nearby stations can display quite distinct behaviors. This impairs the interpolation of the results to other locations in the estuary. Conversely, these erratic characteristics highlight the importance of maintaining a network of stations covering the Elkhorn Slough, for the longest time span possible.

We also reached the above conclusion from the analysis of temperature trends. Here, the two form-free components place northern and southern inland stations on opposite poles, while stations close to the mouth have an even mix of the two behaviors. Southern stations (11, 17, 20 and 23) display a marked cooling in April and warming in December. These trends reduce the annual amplitude over time. This may reflect an increasing tidal flushing over time because of channel erosion (Van Dyke and Wasson 2005). In contrast, northern stations reveal strong warming trends for several months, with summer months and December being the most noteworthy. This warming in the northern part of the Elkhorn Slough may have important biological implications, namely changes in species composition and rates of biochemical processes. The cause for this temperature change is unknown; it may be due to a natural or anthropogenic long-term change in the hydrology of the slough, or to a combination of both.

Our model confirms the relevance of natural forces on temperature in the slough, when the model includes ET_o as a regressor (data not shown). ET_o affects all stations' temperature identically and describes a large fraction of the short-term variability. Thus, the model shows location-independent phenomena contribute to temperature fluctuations as well. The error may contain some natural variability as well, since its covariance structure presents interesting patterns connected nearby stations. In all, our approach demonstrates how temperature trends can be determined in a hydrologically complex estuary.

Seasonal and Long-term trends in Dissolved Oxygen, pH, and Salinity in Elkhorn Slough, California

Authors

Marc Los Huertos, Science and Environmental Policy, California State University, Monterey Bay, 100 Campus Center Drive, Seaside, CA 93955.

Bruno Sanso, Applied Mathematics and Statistics, 1156 High Street, University of California, Santa Cruz, CA 95064.

Introduction

Changes in water composition and consequently, estuarine stability are being seen in coastal estuaries around the world (Altun et al. 2008, Maes et al. 2007, Bauer et al. 2007, Benoit et al. 2006, Dai et al. 2006, Hagy et al. 2004). These parameters depend, in part, on they hydrology and biogeochemistry of an estuary and play an important role in the biological processes and taxa distributions. For example, salinity gradients in estuaries, from freshwater to marine, define marsh vegetation in estuaries based on species tolerance of salt. Nutrient, dissolved oxygen (DO), pH and salinity tend to vary from historical or natural levels demonstrating shifts in estuarine community structure, reduced populations and diminishing habitat (Altun et al. 2008, EPA 2007, Touchette 2007, Sunitha and Jayaprakas 1997, Bauer et al. 2007, Yüksek et al. 2006, Tango et al. 2005, Howarth et al. 2002). Many estuaries in France, China, Australia and the United States are experiencing high influx of nutrients, largely through human activity, which alter the natural state of the complex community structure found in estuaries (Hagy et al. 2004, Colbert and McManus 2003, Howarth et al. 2002, Billen et al. 2001).

Estuaries encompass a complex and versatile habitat for many organisms from benthic invertebrates and phytoplankton to spawning fish (Bauer et al. 2007, Maes et al. 2007, Tango et al. 2005). Low levels of dissolved oxygen (DO) can alter the community structure of phytoplankton sensitive to environmental changes and hinder the migration of fish necessary for spawning (Bauer et al. 2007, Maes et al. 2007, Tango et al. 2005). Declining DO concentrations of 80 μM have been recorded over the past 70 years in the

Canadian St. Lawrence Estuary (Benoit et al. 2006). A continued decline in DO has also been recorded in China's Pearl River Estuary of 100 μmol kg^{-1} (roughly 100 μM) in the past 10 years (Dai et al. 2006).

DO concentrations between 6 and 4.5 mg/L start to effect an organisms growth ability, 4-2 mg/L effect further metabolic interference, 2-0 mg/L is mortal (Gray et al. 2002). Depleted DO levels can lead to drastic changes in biofilm community structure, fish reproduction and the formation of nitrous oxide gas (Bauer et al. 2007, Garnier et al. 2007, Maes et al. 2007). A study by Bauer et al. (2007) found a correlation between low DO concentration with biofilm dominated by ciliates and higher concentrations of DO concentration with biofilm dominated by diatom. Diatoms are primary producers responsible for as much as 30 percent of the world oxygen budget, and a crucial component to aquatic ecosystems. Available DO in water is greatly diminished when diatoms are replaced by heterotrophic ciliates (Bauer et al. 2007). Many fish spawn in or pass through estuaries to spawn. Fish populations have been declining in Europe from hypoxic barriers between fish and historic spawning grounds (Maes et al. 2007). Another implication of low DO concentrations in estuaries is an increased production nitrous oxide contributing to atmospheric green house gasses. The nitrogen cycle uses to oxygen in the denitrification process and if none is available nitrite will be used in its place causing the formation of nitrous oxide gasses (Garnier et al. 2007).

Estuaries are experiencing both increases and decreases in pH values. The pH tolerance for fish is between 5.0 to 8.5 (Moyle and Cech 1996). Organisms are sensitive to changes in pH, it both disrupts cellular function and aid in the process of calcareous and siliceous material dissolution used by animals. In a Turkish lagoon pH values have been rising creating a more basic aquatic environment (Altun et al. 2008). This rise in pH is detrimental to organism development. High pH values enable the denaturation and break down of cell causing death or inability to produce viable offspring (Altun et al. 2007). A study by Lui et al. (2007) found lower pH of between 7 and 6.8 to be associated with higher CO_2 levels and the dissolution of calcium carbonate. Increased aqueous CO2 reacts with water molecules increasing carbonic acid concentrations and then releases a hydrogen atom which decreases pH (Liu et al. 2007, Paz et al. 2007, Zhai et al. 2005).

Salinity changes occur mainly due to fresh water diversion for agricultural, municipal and industrial uses (USEPA 2008). This diversion increases the overall average salinity in estuaries such as San Francisco Bay Estuary (USEPA 2008). Salinity affects the growth and productivity of plants (Touchette 2007). Changes in salinity, like pH, can inhibit growth, decreased fecundity or cause death in estuarine organisms (Sunitha and Jayaprakas 1997). Without internal osmoregulation an organism’s cells can lyse or shrivel depending on salinity concentration (Serkov 2003). Salinity concentrations in estuaries tend to be in between tributaries feeding the estuary and the ocean. Thus, increases salinity concentration may alter nitrification processes. Miranda et al. (2008) concluded the rate of nitrification decreases with a shift in salinity concentrations and change nitrogen species concentrations.

Data Exploration and Modeling Fitting for Dissolved Oxygen

As part of the exploratory process, we found the data to be highly skewed; however we found, after using a cubic root transformation, the response variable approached normality. In addition, significant portions of the data are missing as shown in time series plots (Figure 9). We found the behavior between the tidal and non-tidal sites suggested we consider tidal activity in the model development. Using box plots of the monthly data, we found evidence of a strong seasonal pattern.

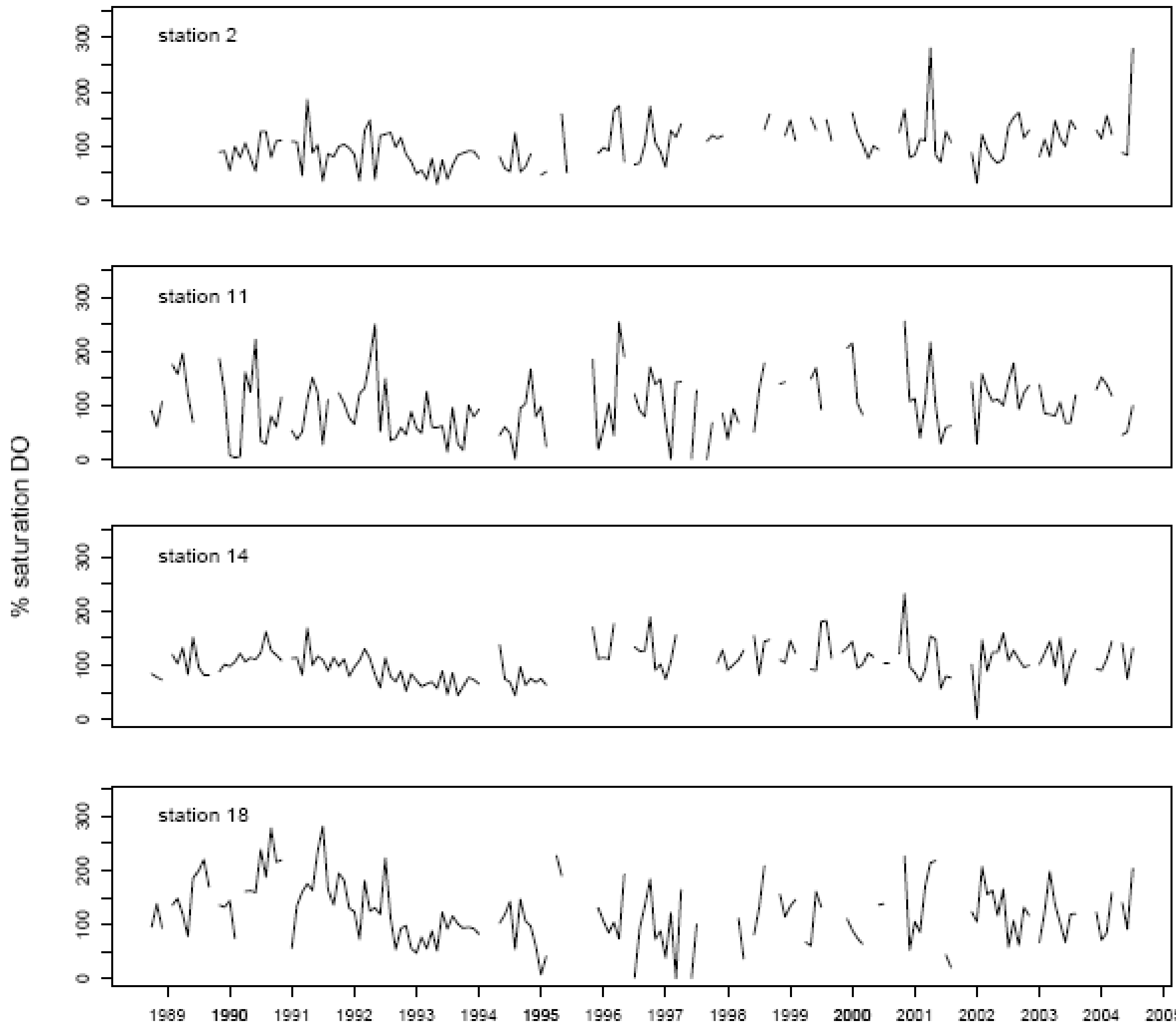

Figure 9. Time series plot of the dissolved oxygen at stations 2, 11, 14, and 18.

The Bayesian periodogram indicates an annual cycle and a peak at 36 months for some stations (Figure 10). Then we fit the following models

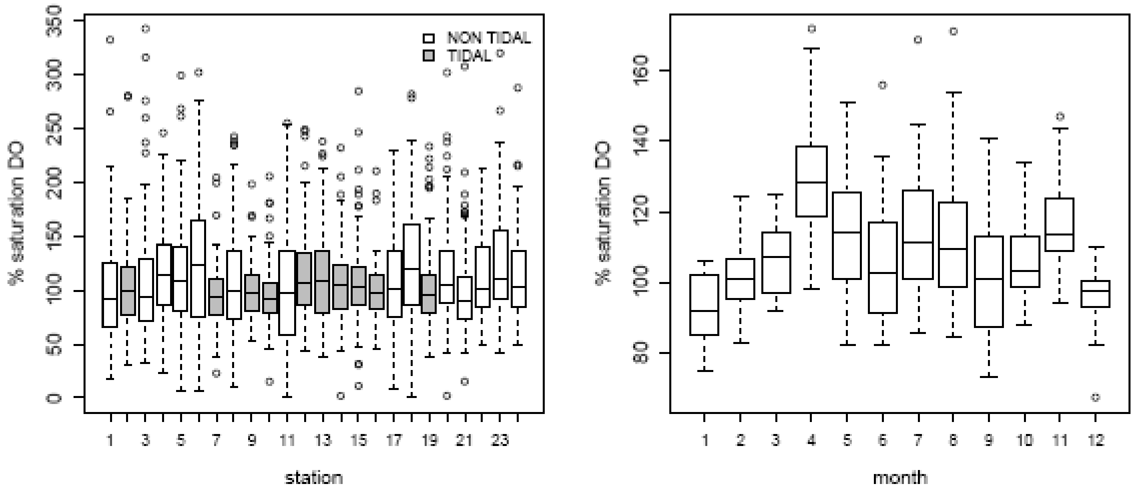

Figure 10. Boxplot of dissolved oxygen for each station (left panel) and for each month (right panel). White boxplots correspond to non tidal stations and gray boxplots to tidal stations in the left panel.

The Bayesian periodogram indicated an annual cycle and a peak at 36 months for some stations. We used the cubic root transformation to get normality of the data. We fit a model for each station considering two different slopes plus a seasonal component with peak at 12 and 36 months following the periodogram.

We used the following model:

Equation 3

$$y_t = a + b \cdot t + c \cdot (t - 60) \cdot X + d \sin(2\pi \cdot t / 12) + e \cos(2\pi \cdot t / 12) + \varepsilon_t$$

where X = 1, if $t > 60$ and X = 0, if $t \leq 60$, $y_t = (DO)^{1/3}$, a represents the level, *b* the trend coefficient if $t \leq 60$, $b + c$ the trend coefficient if $t > 60$ and *d* and *e* represent the periodical coefficients. We consider λ = 12 and λ = 36. The parameters *d* and *e* are not significant for most stations implying that there is no periodical component. The trend coefficient, *b*, is significant and negative for most of the stations. In other words, DO is decreasing until t = 60 (Figure 11 Right Panel).

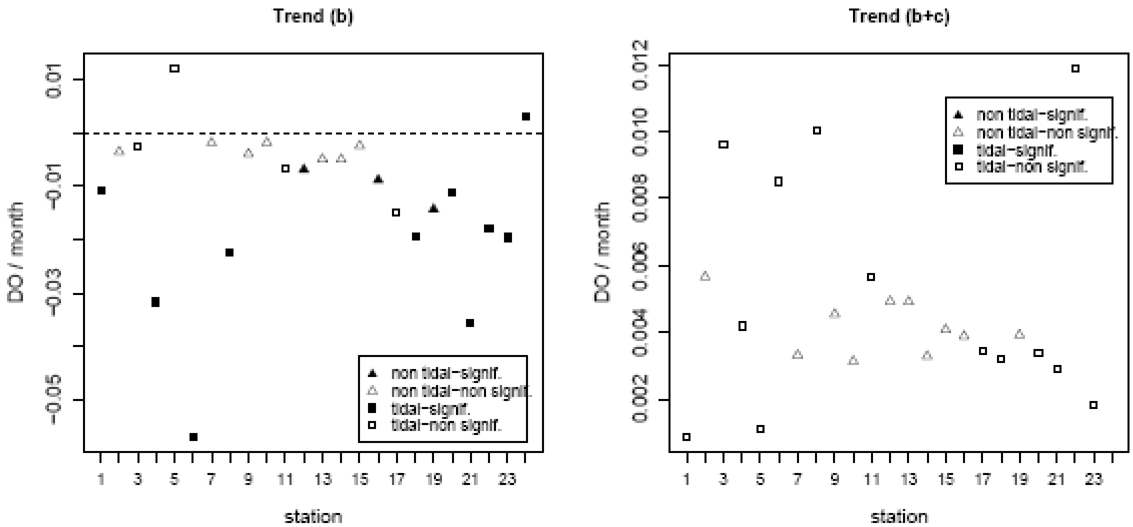

Figure 11. Trend coefficients of dissolved oxygen for each station. If t <= 60, *b* is the trend coefficient otherwise *b* + *c* is the trend coefficient. Triangles correspond to non tidal and squared to tidal station. Filled and open symbols correspond to significant and non significant coefficients, respectively.

Data Exploration and Modeling fitting of pH

Our exploratory data analysis began with a time series plot and Bayesian periodogram at the 24 stations. The boxplot of pH at each station shows there is some difference between tidal and non-tidal stations (Figure 13).

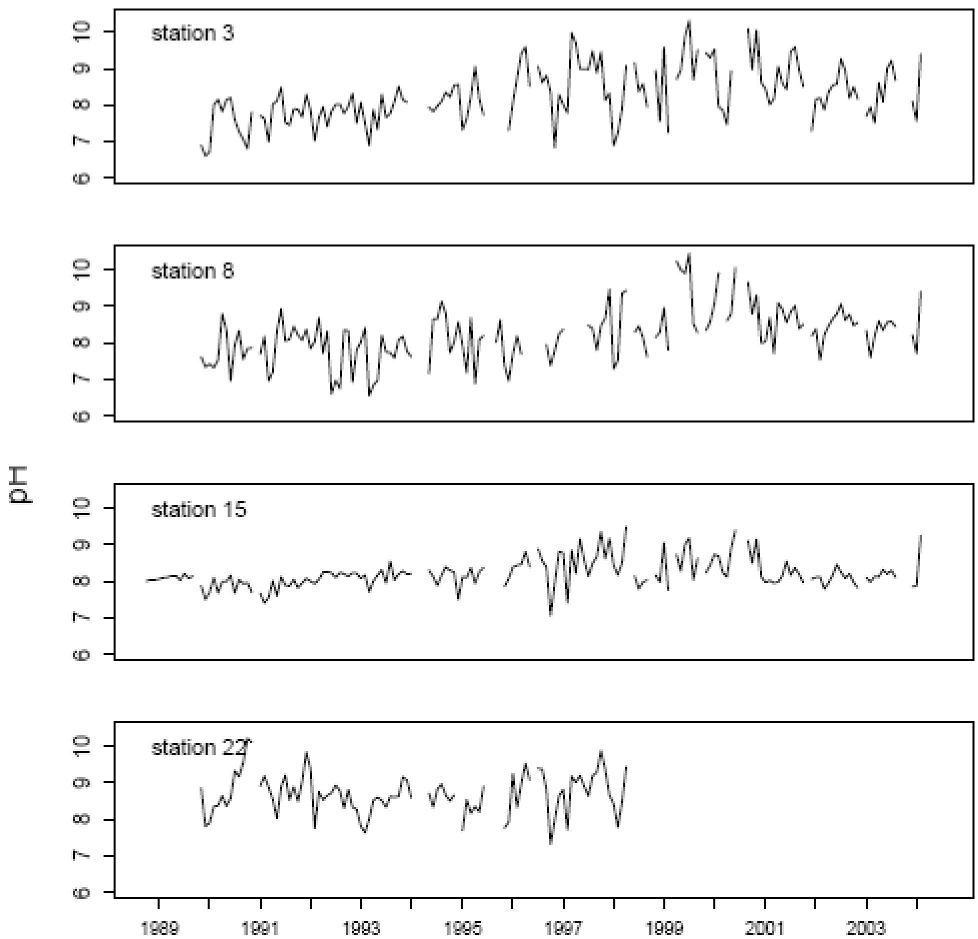

Figure 12. Time series plot of pH at stations 3. 8, 15, and 22.

The percent of missing values varies between 11.6% (station15) and 18.9% (station22). The boxplot of monthly averages split by tidal and non-tidal levels in April and lower levels in August. The tidal stations have higher values Ph than non-tidal ones (Figure 13).

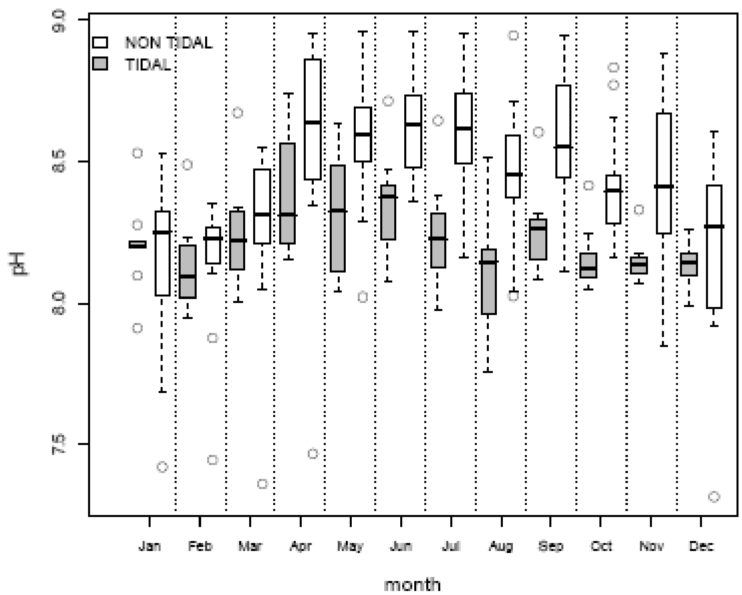

Figure 13. Boxplot of pH considering month average split by tidal and non tidal stations. Open boxes corresponds to non tidal stations and grey box plots to tidal stations.

We fit a multivariate regression model for each station considering precipitation, salinity, temperature and monthly effects plus a trend:

Equation 4

$$pH_t = \mu + \alpha_1 \cdot ppt_t + \alpha_2 2 \cdot sal_t + \alpha_3 \cdot temp_t + \beta t + \gamma_m X_m + \varepsilon_t, \varepsilon_t \sim N\left(0, o^2\right)$$

where ppt is the precipitation, sal is the salinity, temp is the temperature, $t = 12(y - y_1) + m$, with $y_1 = 1988$ and y and m are the current year and month respectively, γ_m is the monthly effect and Xm is 1 if m is the current month and 0 otherwise. We are considering January as the baseline month. Then, $\gamma_m = (\gamma_{Feb}, \gamma_{Mar}, \ldots, \gamma_{Dec})$.

Figure 14 shows the posterior mean and 95% credible interval for the precipitation and temperature coefficients. Precipitation is significant for half of the stations. For example, at station 4 the coefficients are positive what means more precipitation increased the level of pH. The opposite is observed at other stations for example at stations 17, 20, and 21. The temperature is significant and positive for most of the stations. The monthly effect is significant for some stations. For example, at station 5 the effect of February, April, May, June and November compared to January are significant (Figure 15).

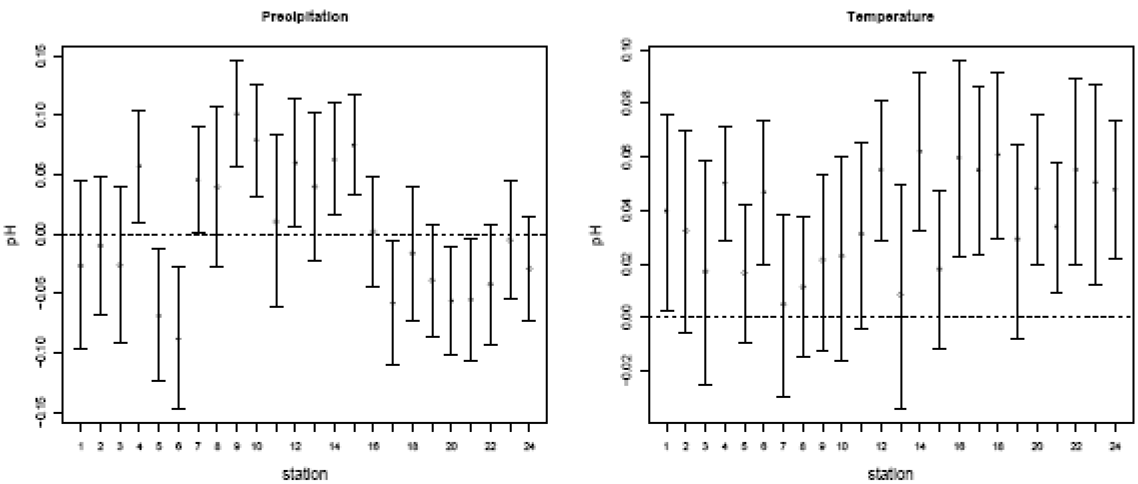

Figure 14. Posterior means and 95% probability intervals for the coefficients of precipitation (left panel) and temperature (right panel) for each station.

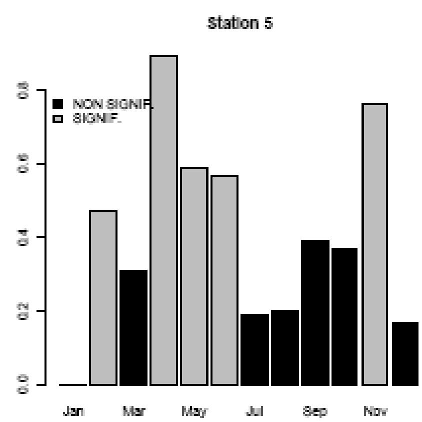

Figure 15. Monthly effect relative to January for station 5.

Data Exploration and Model Fitting of Salinity and Conductivity

After some exploratory data analysis, we used a square root transformation for salinity. The time series plot shows we have different behavior for the stations. We compared salinity in tidal and non-tidal (including muted tidal) stations and find that the non-tidal sides were much more variable (Figure 16). Figure 17 uses the square root of salinity, which create a distribution that approaches a normal distribution. Then we made the dendogram to create to determine which sites were similar to each other with respect to salinity. Basic on Figure 18, we created two groups and split each group in tidal and non-tidal. We fitted different models for each group.

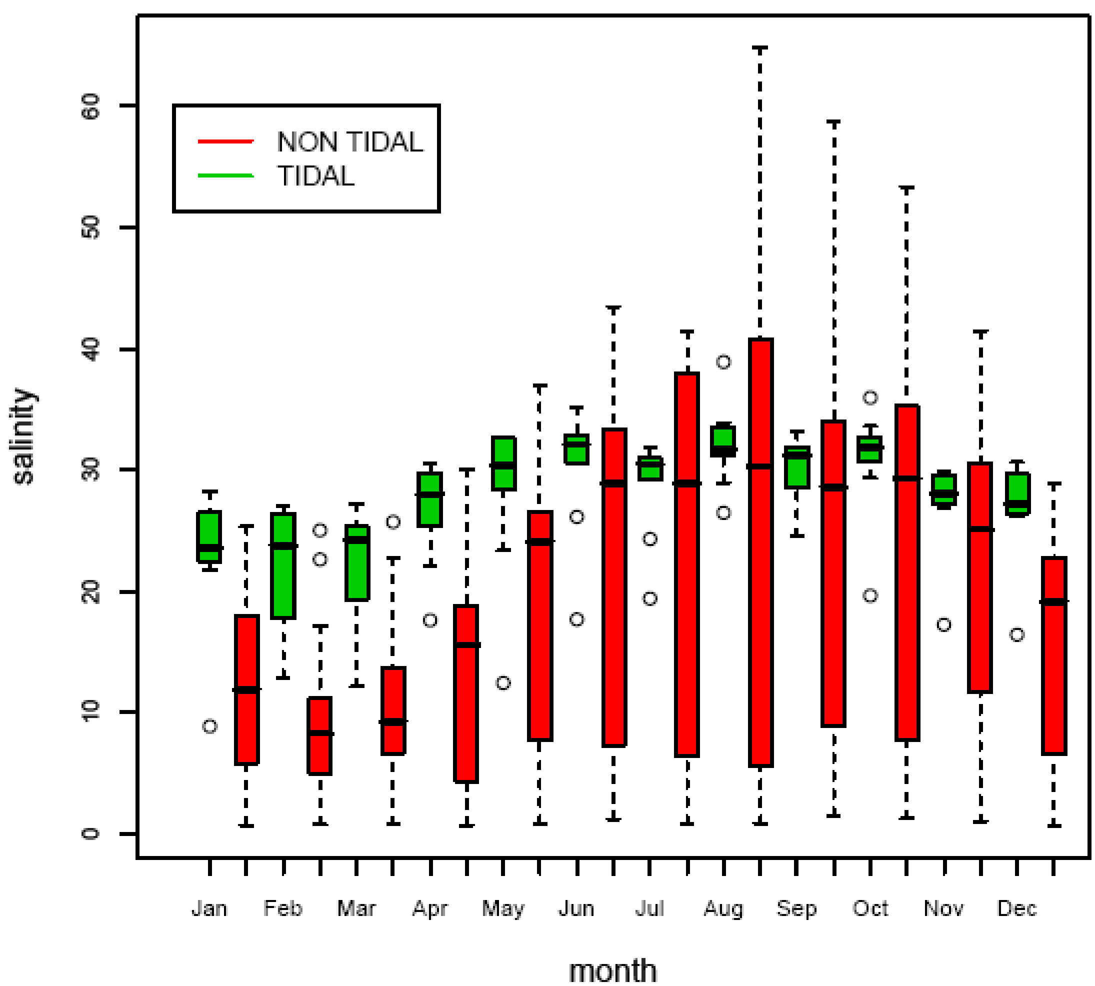

Figure 16. Salinity measurements for tidal and non tidal stations for each month.

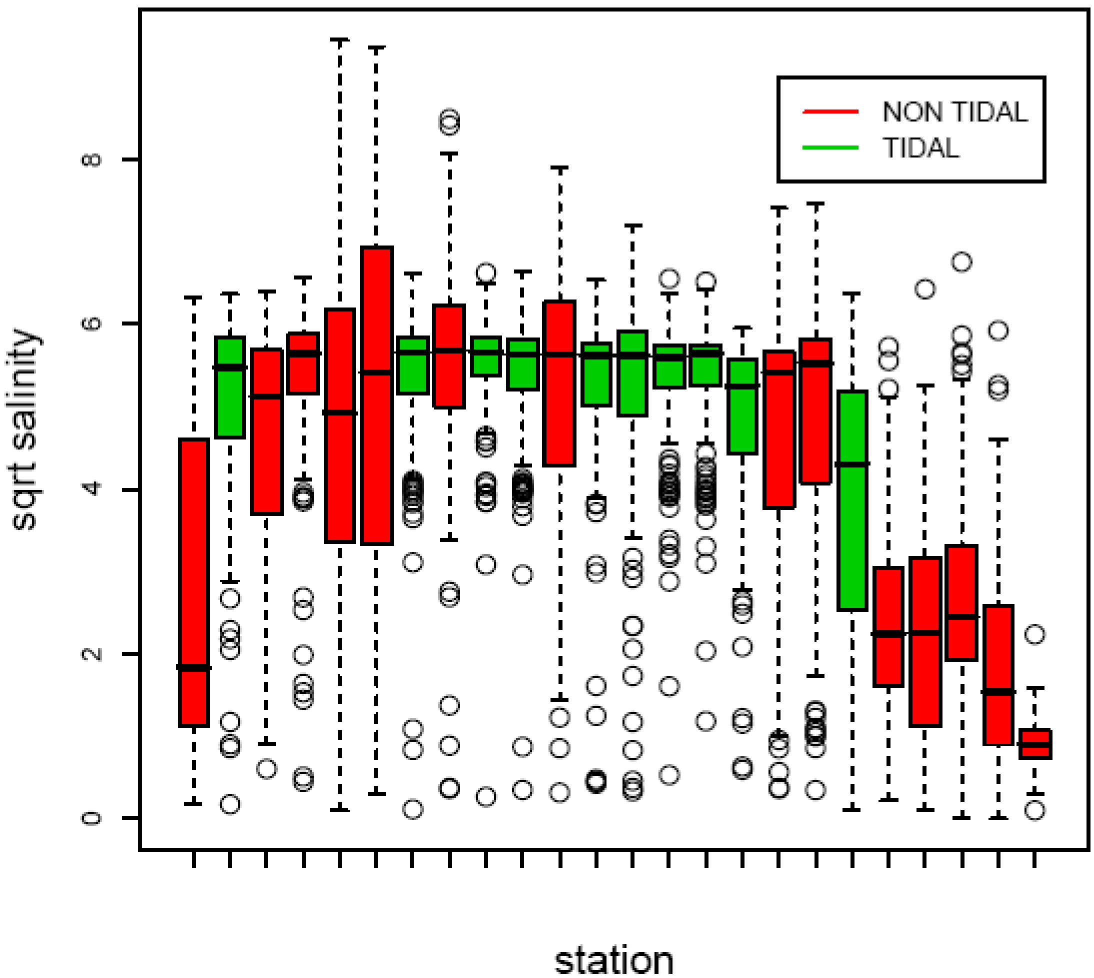

Figure 17. Salinity reading by station.

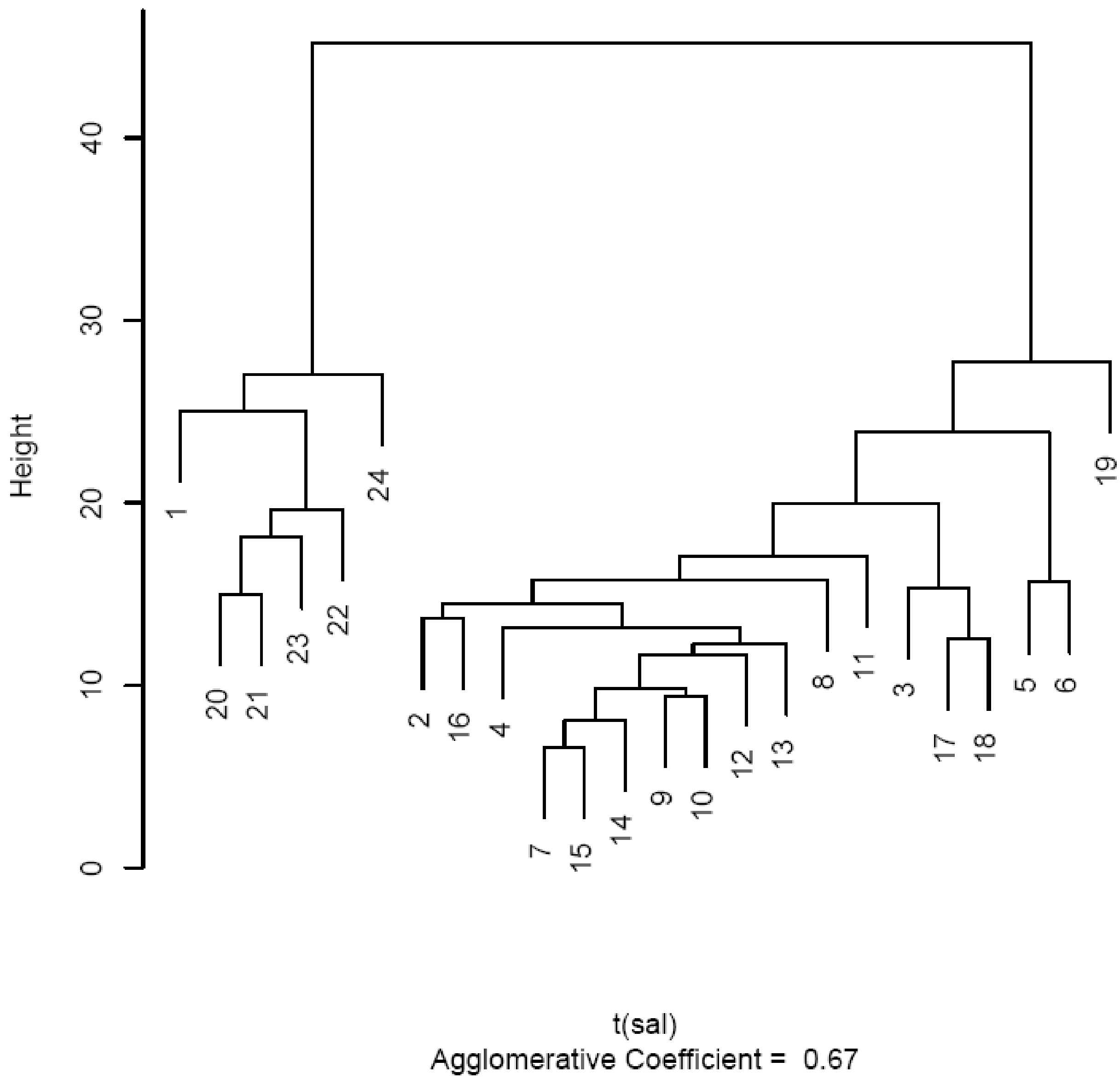

Figure 18. Dendogram of stations using salinity to differentiate each station.

We used Equation 5 to model the tidal sites and Equation 6 for the non-tidal sites. For the non-tidal sites, we include a regime change function that allows for seasonal shifts in salinity, presumably due to freshwater inflows that are limited to the rainy season.

Equation 5

$$y_t = \mu_t + \varepsilon_t$$
$$\mu_t = X_t \theta$$
$$\varepsilon_t = \sum \phi_j \varepsilon_{t-j} + \upsilon_t \sim N\left(0, \sigma^2\right)$$

Equation 6

$$y_t = \mu i_t + \varepsilon_t, i = 0,1$$
$$\mu_{it} = X_t \theta_i$$
$$\varepsilon_t = \sum \phi_j \varepsilon_{t-j} + \upsilon_t \sim N\left(0, \sigma^2\right)$$
$$P\left(I_t = 1\right) = p_t), p_t = \frac{\exp\{\alpha + \beta r_t\}}{1 + \exp\{\alpha + \beta r_t\}}$$

Where X_t = (1, cos(2π *t*/12), sin(2π*t*/12),*t,r*t,h_t) and t_i = (m_i,a_i, b_i, c_i, d_i, e_i) for Group 1a and 2a and X_t = (1,cos(2π *t*/12,sin(2π*t*/12,*t*,r_t) and t_i = (m_i,a_i,b_i,c_i, d_i) for Group 1b and 2b.

The structure mean is, for the most part, the same for all groups. We have a level, an annual cycle, trend, precipitation and tide height for tidal groups. The error is modeled using an autoregressive process of order *p*(AR(*p*)). To verify the order process we fitted the model with different orders and used the Gelfand and Gosh criterion to make a decision. We have different orders for the group 1. The trend and precipitation coefficients are significant.

The time series plot for group 2 indicates a presence of 2 regimes. Then we used a regime switching model. The probability of changing regime is $P(I_t=1)=p_t$ with $I_t=1$

representing low salinity. The switching is given by precipitation, $pt = (\exp(\alpha+\beta r_t))/(1+\exp(\alpha+\beta r_t))$. It means when we have high levels of precipitation we have low levels of salinity.

The structure mean is, basically, the same for all groups. We have a level, an annual cycle, trend, precipitation and tide height for tidal ones. The error is modeled using an autoregressive process of order p (AR(p)). To verify the order process we fitted the model with different orders and used the Gelfand and Gosh criterion to make a decision. We have different orders for the group 1. The trend and precipitation coefficients are significant. The time series plot for group2 indicates a presence of 2 regimes. Then we used a regime switching model. The probability of changing regime is $P(It = 1) = pt$ with $It = 1$ representing low salinity. The switching is given by precipitation, $pt = \exp\{\alpha+\beta rt\}$. It means when we have high levels of precipitation we have low $1+\exp\{\alpha+\beta rt\}$ levels of salinity. The switching regime model seems to fit well on the data. The posterior mean has the similar behavior to observed data and capture the low salinity peaks happening over the time. For some stations like station 4, the classification plot is very clear (low and high salinity). The autoregressive order chosen was p=1 according of Gelfand and Gosh criterion.

Table 9. Gelfand and Gosh Criterion—Model 1

Table 1: Gelfand and Gosh Criterion - Model 1

Station	p=1	p=2	p=3	p=4	p=5
1	**429.98**	430.18	432.92	434.99	
19	447.02	448.86	451.22	450.75	**434.92**
20	269.88	270.74	256.64	253.49	**249.58**
21	281.87	277.99	**276.37**	277.34	279.23
23	290.54	**284.15**	285.23	287.52	287.97

Discussion

Spatial Patterns in Water Quality Parameters

Estuaries have strong spatial gradients largely driven by the mixing patterns of freshwater and saltwater. Elkhorn Slough has a relatively small watershed area and limited freshwater inputs during the summer months. Prior to our study, we believed the spatial pattern in variability would be easy to explain in relation the relative connectivity the water had to the main channel, thus seawater of the Monterey Bay. Salinity and temperature followed this pattern well and reflected fresh-seawater gradients and seasonally driven changes in flow and evaporation.

Salinity and conductivity was difficult to work with because there were some data quality problems. These problems included a number of missing points and the lack of linearity between the two measures. The same instrument generally collects measurements, where salinity is calculated from temperature and conductivity. However, we found the data do not always follow the theoretical equations. In addition, recorded salinities appear to be excessive at times, suggesting calibration or recording errors.

The spatial pattern of pH suggests the water entering the slough from the north is less alkaline or better buffered, especially in the winter months. We saw that Carneros Creek had the lowest pH of the sampling sites (median=7.2) while the Salinas River had a pH of 8.3.

Overall, dissolved oxygen levels were high at all sites. However, we noted increasing concentrations at several sites indicate eutrophic conditions, and possible depression of nighttime DO concentrations. This may have important implications for slough biota. In future, work we suggest a better understanding of the algae blooms, diel dissolved oxygen concentrations, and nutrients be a research priority.

Dissolved oxygen concentrations are a balance of water column photosynthesis, respiration and temperature-driven solubility of oxygen in water. The lowest concentrations occurred in the central part of the slough (Reserve Marsh, Central

Marsh) and this area had some of the highest summer time temperatures. It is not clear if the dissolved oxygen concentrations differences are driven by biological processes. To better assess this, future work will include diel dissolved oxygen sampling and converting dissolved oxygen concentrations to percent saturation.

The Azevedo Ponds and several areas have limited to no tidal exchanges. The South Azevedo Pond, characterized as ‘hyperventilating’ (i.e., hypereutrophic) had dramatic shifts in DO between 0.16 and 17.5 mg/L (Beck and Bruland 2000). Warm water temperature, temporary lack of tidal mixing, elevated nutrient concentrations create these conditions in this small pond. The diel cycle drives not only DO but also drives nitrogen, phosphorus, iodine, manganese, and iron. DO at this site was among the highest recorded, but median DO measurements were higher at other sites, e.g. North Marsh, Moss Landing (north), Potrero Road (south), Salinas River Lagoon and Bridge, and Tembladero Slough. Additionally, only a few sites in the central slough and near the mouth were statistically distinguishable in their maximum DO from the Lower Azevedo Pond. This suggests hypereutrophic conditions maybe more widespread in the slough. However, the maximum temperatures in the Azevedo Ponds (along with the north marsh) were significantly higher than other sites. These maximum temperatures are the result of limited tidal mixing and relative shallow conditions.

Seasonal and Long-term Trends in Dissolved Inorganic Nutrient Concentrations in Elkhorn Slough, California

Authors

Lelys Guenni, Universidad Simón Bolívar, APDO. 89.000. Caracas 1080A. Venezuela.

Bruno Sansó, Applied Mathematics and Statistics, 1156 High Street, University of California, Santa Cruz, CA 95064.

Marc Los Huertos, Science and Environmental Policy, California State University, Monterey Bay, 100 Campus Center Drive, Seaside, CA 93955.

Abstract

We consider, in this research, data of dissolved inorganic nutrient concentrations (ammonium (NH_4^+), ortho-Phosphorous (PO_4^-) and nitrate (NO_3^-) concentrations from 24 locations for over sixteen years in the Elkhorn Slough National Estuary. The slough is located in the Monterey Bay area in central California, USA. We develop a statistical model to quantify concentration variation due to trends and seasonality. Initial exploratory data analysis revealed high variability among locations and the presence of outliers for some locations. These outliers are possibly due to observational errors. We observed different behaviors for spatially proximate stations. We propose a model consisting of trend and seasonal components where the errors follow an autoregressive process. An additive observational independent error is also included in the model structure. We use a Bayesian approach to explore the posterior distribution of the parameters using WinBUGS. Some stations have a marked seasonal pattern; however, neighboring stations can have substantially different behaviors. We found some stations demonstrated significant increasing trends in nutrient concentrations. Key words: Bayesian Modeling; Trend Analysis; Water Quality data; Observational Errors.

Introduction

Estuaries are the most highly anthropogenically impacted habitat of all habitat types (Edgar et al. 2000), yet estuaries host rich, distinctive biodiversity including migratory shorebirds, and nursery fishes among others (Laprise and Dodson 1994; Whitfield

1994; Price 2002). Although there are a number of threats to these important habitats, elevated nutrient inputs increase the risk of eutrophication, which is a ubiquitous problem in estuarine habitats (National Research Council 1993). More than one half of estuarine habitats are eutrophic with intense nutrient loading leading to blooms and anoxia (Sanger et al. 2002). Eutrophic conditions produce a decline in estuarine biodiversity, a reduction of healthy fisheries, the loss of quality larval nursery habitat, and available food for shorebirds (Baden et al. 1990; Pihl et al. 1991; Burkholder et al. 1992; Nixon 1995; Rabalais et al. 1996).

A recent synthesis of water quality at 22 estuaries nationwide revealed most West Coast estuaries rarely suffer from these problems (Wenner and Geist 2001). However, Elkhorn Slough and Tijuana Estuary have been identified as the most eutrophic estuaries in U.S. NOAA designated network of National Estuarine Research Reserve systems. Significant portions of Elkhorn Slough have elevated nutrient concentrations (Chapin et al. 2004; Caffrey et al. 2002; Caffrey et al. in press).

Changes in water composition and consequently, estuarine stability are being seen in coastal estuaries around the world (Altun et al. 2008, Maes et al. 2007, Bauer et al. 2007, Benoit et al. 2006, Dai et al. 2006, Hagy et al. 2004). Nutrients, dissolved oxygen (DO), pH and salinity tend to vary from historical or natural levels demonstrating shifts in estuarine community structure, reduced populations and diminishing habitat (Altun et al. 2008, EPA 2007, Touchette 2007, Sunitha and Jayaprakas 1997, Bauer et al. 2007, Yüksek et al. 2006, Tango et al. 2005, Howarth et al. 2002). Many estuaries in France, China, Australia and the United States are experiencing high influx of nutrients, largely through human activity. This activity alters the natural state of the complex community structure found in estuaries (Hagy et al. 2004, Colbert and McManus 2003, Howarth et al. 2002, Billen et al. 2001).

Elevated nutrients such as nitrate, phosphate, and ammonia lead to excessive photosynthetic algal growth (Turner et al. 2008, Maes et al. 2007, Liu et al. 2007). Excess algal growth or blooms have a cascading effect causing oxygen depletion or hypoxic areas during the decomposition process, removing oxygen necessary to support virtually all life in the estuarine ecosystem (Altun et al. 2008, Bauer et al. 2007, Tango et al. 2005). There has been a trend of decreasing DO concentrations over the past forty year in some estuaries (Benoit et al. 2006, Dai et al. 2006, Hagy et al. 2004). Low levels of DO in conjunction with ever-increasing levels of atmospheric carbon dioxide tend to decrease aquatic pH levels (Liu et al. 2007). In other areas increased pH levels have occurred possibly due to excessive algal blooms (Altun et al. 2008).. Estuaries are also experiencing reduced fresh water input from redirecting water for municipal and agriculture use. This redirection of fresh water causes less dilution of estuaries and increased salinity (EPA 2007).

For the past 20 years, the EPA has been practicing restoration and protection for 28 estuaries for the EPA's National Estuary Program (NEP). In 1990, the EPA began to compile the data obtained through the NEP and other data to include many of the nation's estuaries and published in the National Coastal Conditions Report. Despite restoration efforts, the nations estuaries have maintained their fair condition rating from 1990 to 2000. Of the 28 estuaries in the National Estuary Program 28 are experiencing habitat loss, 25 a decline or loss of species, 21 high nutrient loading, 11 fresh water input, 5 hypoxia (EPA 2007).

Nitrate and Phosphate concentrations have been continually rising in the Seine River Estuary, France (Billen et al. 2001). Ammonia/ammonium toxicity occurs when acidic pH is found with high salinity and basic pH is found with low salinity (Eddy 2005).

The Gulf of Mexico has experienced increasing nutrient input from the Mississippi River watershed over the past 40 years causing a massive hypoxic and sometimes anoxic zone killing fish and putting great stress on the fisheries and the ecosystem of the Gulf (Turner et al. 2008). Nutrients including nitrate, phosphate and ammonia are introduced to watershed systems from fertilizers, manure and urine from farms and feed lots, wastewater effluent, detergents and other urban runoff (Brown 2001, Howarth et al. 2002, EPA 2007). High nutrient loads are the beginning of a succession of problems found in estuaries (Turner et al. 2008, Hagy et al. 2001). The first step in the succession is algal blooms, reducing light penetration in the aquatic estuarine ecosystem (Turner et al. 2008). Algal blooms lead to changes in DO concentrations. With high concentrations of DO in the euphotic zone and a massive consumption of DO, as the algae falls and decomposes, in the benthic environment (Turner et al. 2008). Many organisms are sensitive to changes in DO. High concentrations can lead to oxygen dissolution forming bubbles, which block blood flow in fish, and low concentrations deprive fish of oxygen. Both situations can be fatal. Depleted DO alters the nitrification process and can lead to a decrease in pH levels (Garnier et al. 2007). Finally, nutrient loading is largely accompanied by freshwater diversion preventing freshwater from entering estuaries and thereby increasing salinity concentrations.

The succession process can also lead to a shift in the composition of organisms naturally found in the ecosystem (Bauer et al. 2007, EPA 2007, Maes et al. 2007). Yet another implication of increased nutrient loading is increased nitrous oxide levels adding to greenhouse gases in the atmosphere helping to continue the global climate change (Garnier et al. 2007, Barnes and Owens 1998).

High turbidity tends to accompany over stressed estuarine systems, which lowers the light entering the water (Miranda et al. 2008). Light is essential for photosynthesis and uses ammonium in this process, therefore ammonium concentrations increase in the water column and toxicity becomes of concern with higher turbidity (Miranda et al. 2008). Systems in stress already have difficulty removing ammonium from the water and when added it further intensifies the possibility of ammonium toxicity posioning of the organisms.

Elkhorn Slough was designated a National Estuarine Research Reserve (NERR) in 1979. The slough plays an important ecological role with a variety of habitats including extensive marshes and mudflats. These habitats are rare along the central coast of

California. However, similar to other estuaries, the hydrology is spatially and temporally complex, thus broad surveys fail to capture the importance of this variability. Furthermore, it is a challenge to develop and maintain monitoring programs to capture this variability while developing record lengths long enough to discern water quality trends in the context of seasonal variation. As part of the goals to conserve and restore of estuarine habitats, staff and volunteers associated with Elkhorn Slough began actively monitoring water quality in the slough beginning in 1988. However, there have been no careful examinations of the data, to determine if temporal trends of nutrient concentrations exist.

For the analysis of dissolved nutrients, we consider if there are significant long-term trends in dissolved nutrient concentrations during the period 1988—2004 and whether these changes occur similarly across the reserve. We began with an exploratory analysis using a non-parametric test for a monotonic trend using a Seasonal Mann-Kendall (SK) test. We followed this by developing a Bayesian time-series analysis. Finally, we compare the results of the two approaches and interpret them in the context of characteristics of land use and tidal exchange in the slough.

Exploratory Analysis

Open-source R software was used to determine summary statistics including distribution-free confidence intervals and medians (CRAN 2008). To explore site-specific, long-term trends, we used the Seasonal Mann-Kendall (SK) test and the Kendall package.. This is a distribution free (non-parametric) test. The test partitions data into seasonal categories, using months as seasons (Helsel and Hirsch 1992). Because of changing laboratory methods (and detection limits), we ran the tests three times for each site and parameter. Values below the detection limit were: 1) zero; 2) one half of the detection limit, and 3) equal to the detection limit.

Ammonium concentrations ranged from N.D. (non detect) to 12.4 and a median of 0.1 mg N/L (0.18 mg N/L mean). Eleven sites had a significant trend where 6 sites were increasing and five were declining when the MDL (minimum detection limit) was substituted for N.D. value (Table 9). These results changes when 0.5 MDL and zero are substituted for N.D. values. Only eight sites showed a significant trend for the 0.5 MLD method, where 4 sites were increasing and 4 sites were declining.

Phosphate concentrations ranged from N.D. to 8.0 and a median of 0.14 mg P/L (0.29 mg P/L mean). Fourteen sites had a significant trend where seven sites were increasing and seven were declining when the MDL was substituted for N.D. value (Table 10). Only one site changed with the N.D. substitution method used. This may be a site with the lowest Kendall's Tau value indicating the potential for increasing concentrations.

Nitrate concentrations range from N.D. to 90 mg N/L across the sites during the study period. The median concentration was 0.54 mg N/L, while the mean was 4.4 mg N/L, demonstrating a highly skewed data set. Between eight or nine sites had evidence of a trend in nitrate concentrations, where five have been increasing and three or four have declined (Table 8).

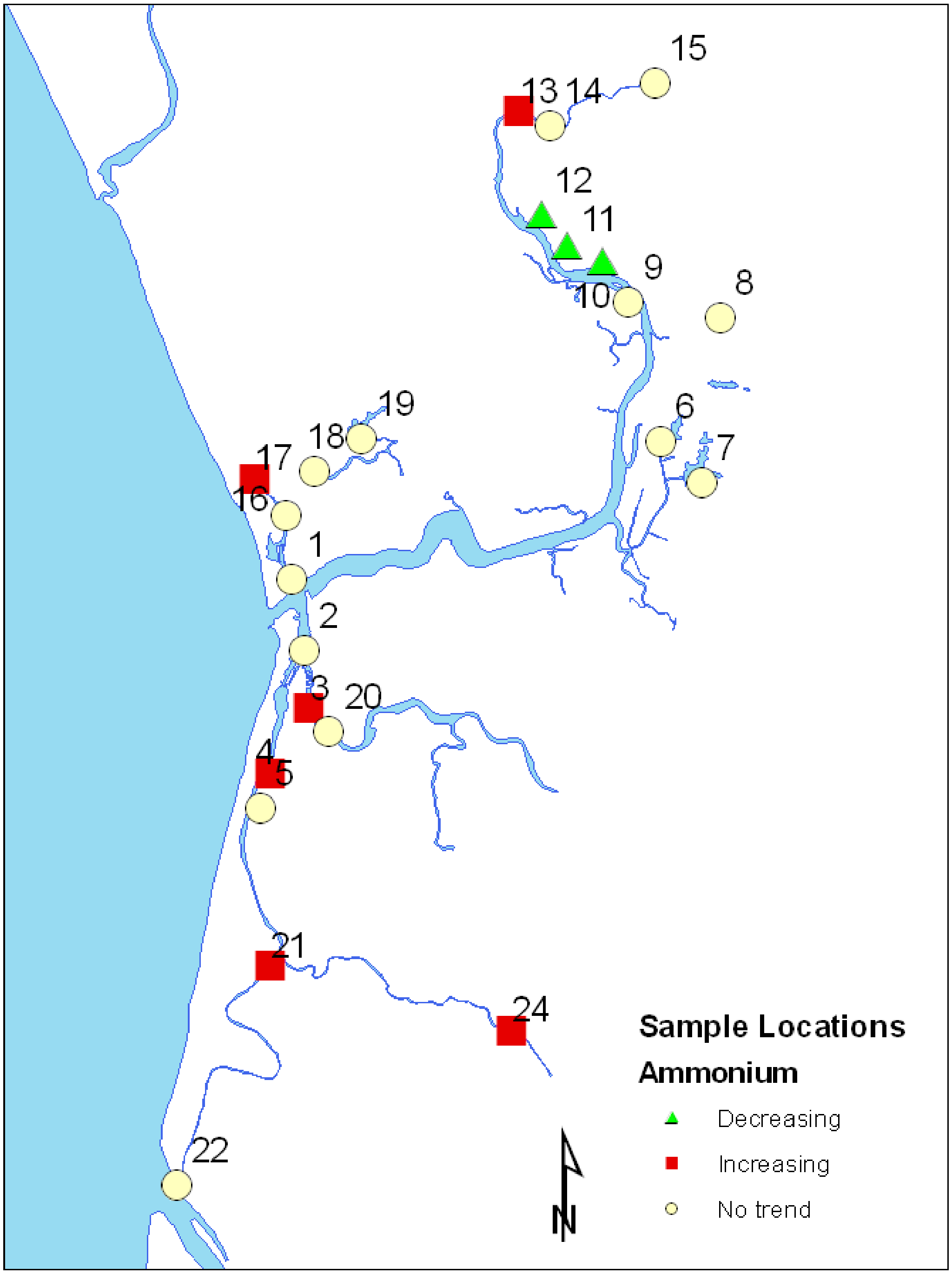

Figure 19. Ammonium trends in Elkhorn Slough based on Seasonal Kendall test.

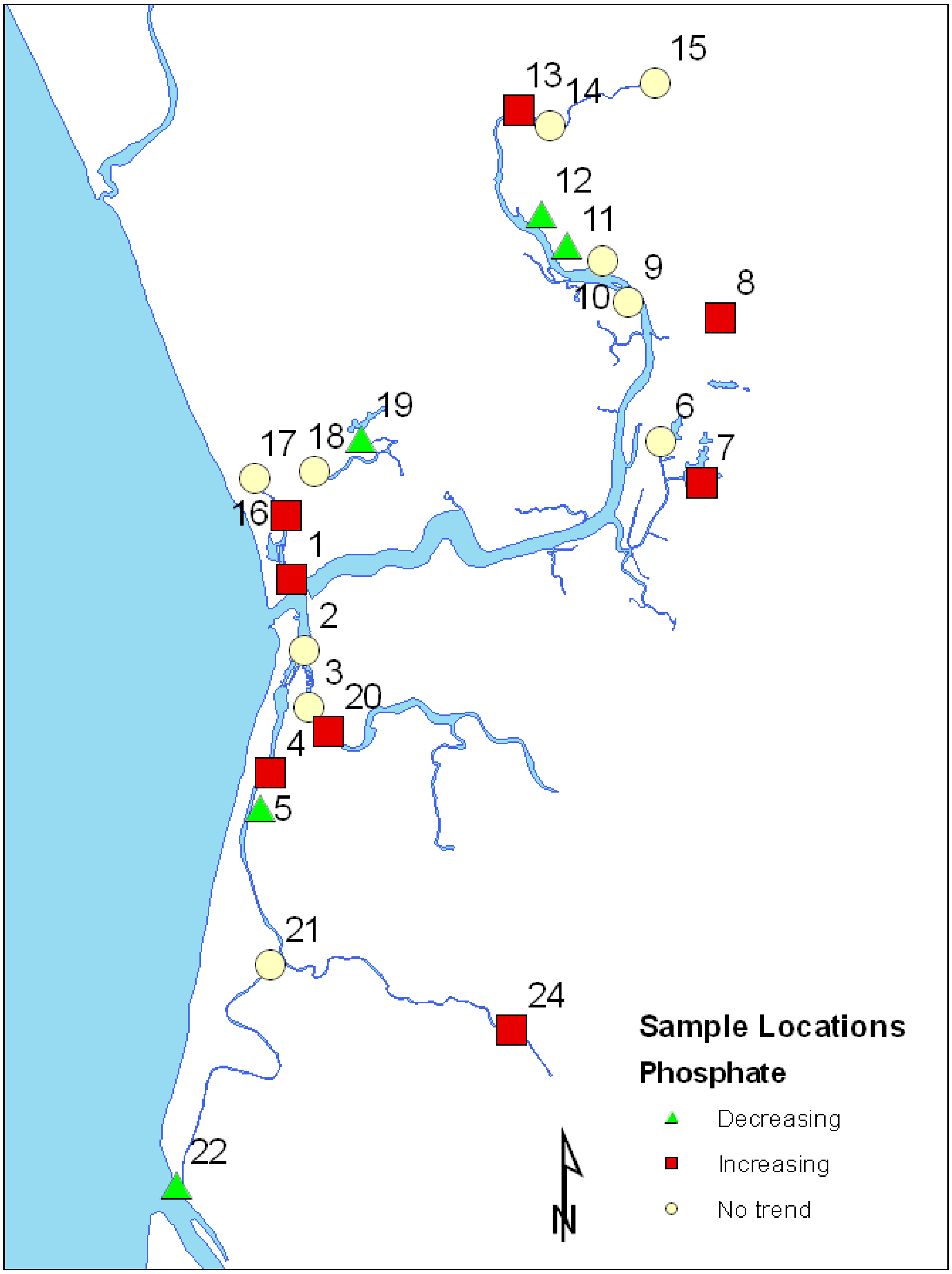

Figure 20. Phosphate trends in Elkhorn Slough based on Seasonal Kendall test.

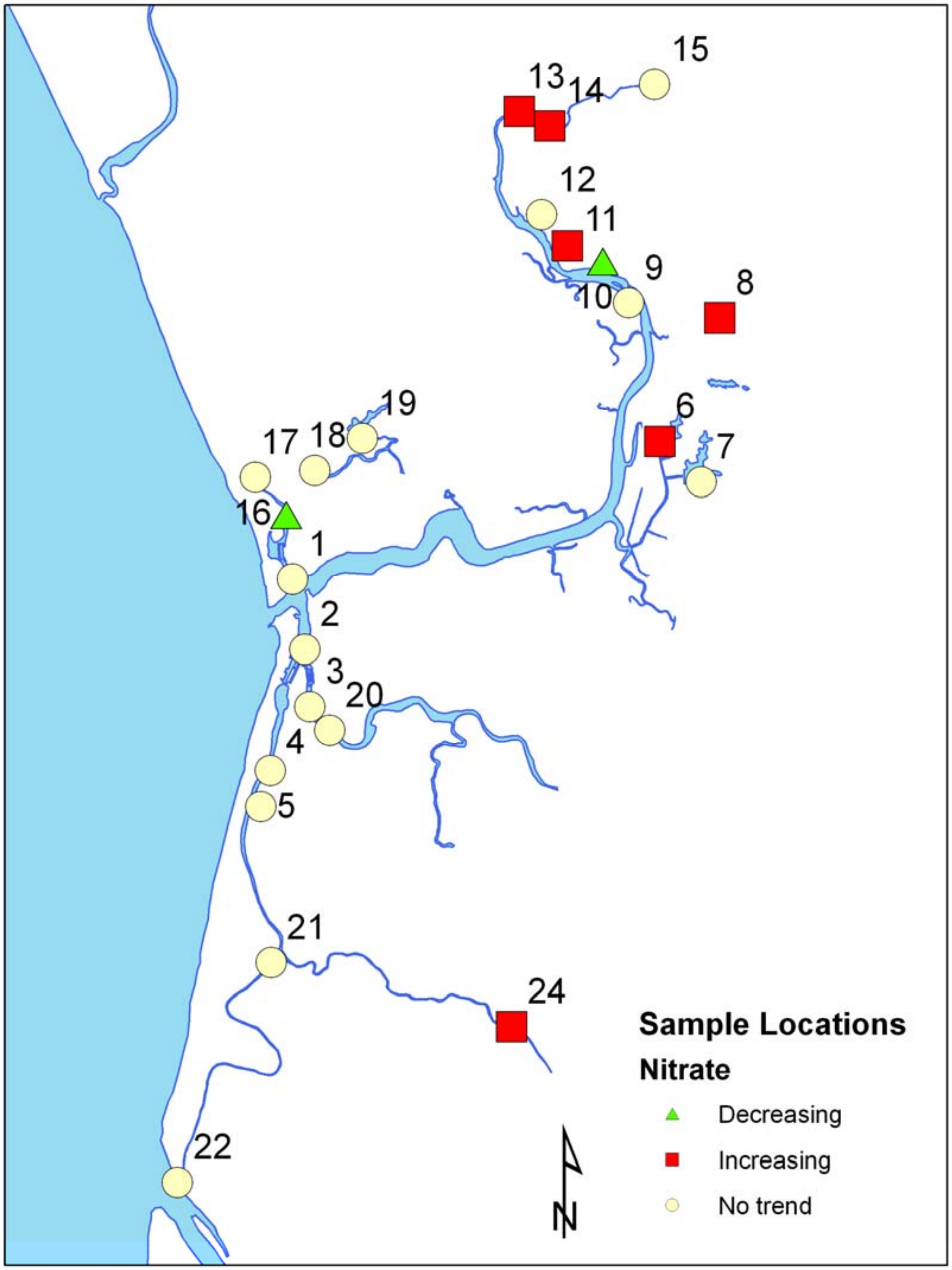

Figure 21. Nitrate trends in Elkhorn Slough based on Seasonal Kendall test.

From graphical exploration of the time series, the presence of increasing or decreasing trends is not obvious for many locations. Figures 22, 23, and 24, show the time series for locations 17, 18, 19 and 20 for ammonium, ortho-Phosphorous, and nitrate respectively. Data collected at other stations show similar features. By inspection of the time series plots some outliers are apparent at some locations, as for example location 3 for nitrate after year 2000, and locations 23 for ammonium and 13 for phosphorous towards the end of the observing period (Figures not shown). We also observed high peaks for locations 5, 6 and 11 for ammonium between 1995 and 1998. Trends for ortho-P in locations 5, 6 and 11 seem to be decreasing. Overall, we observe a marked variability among locations.

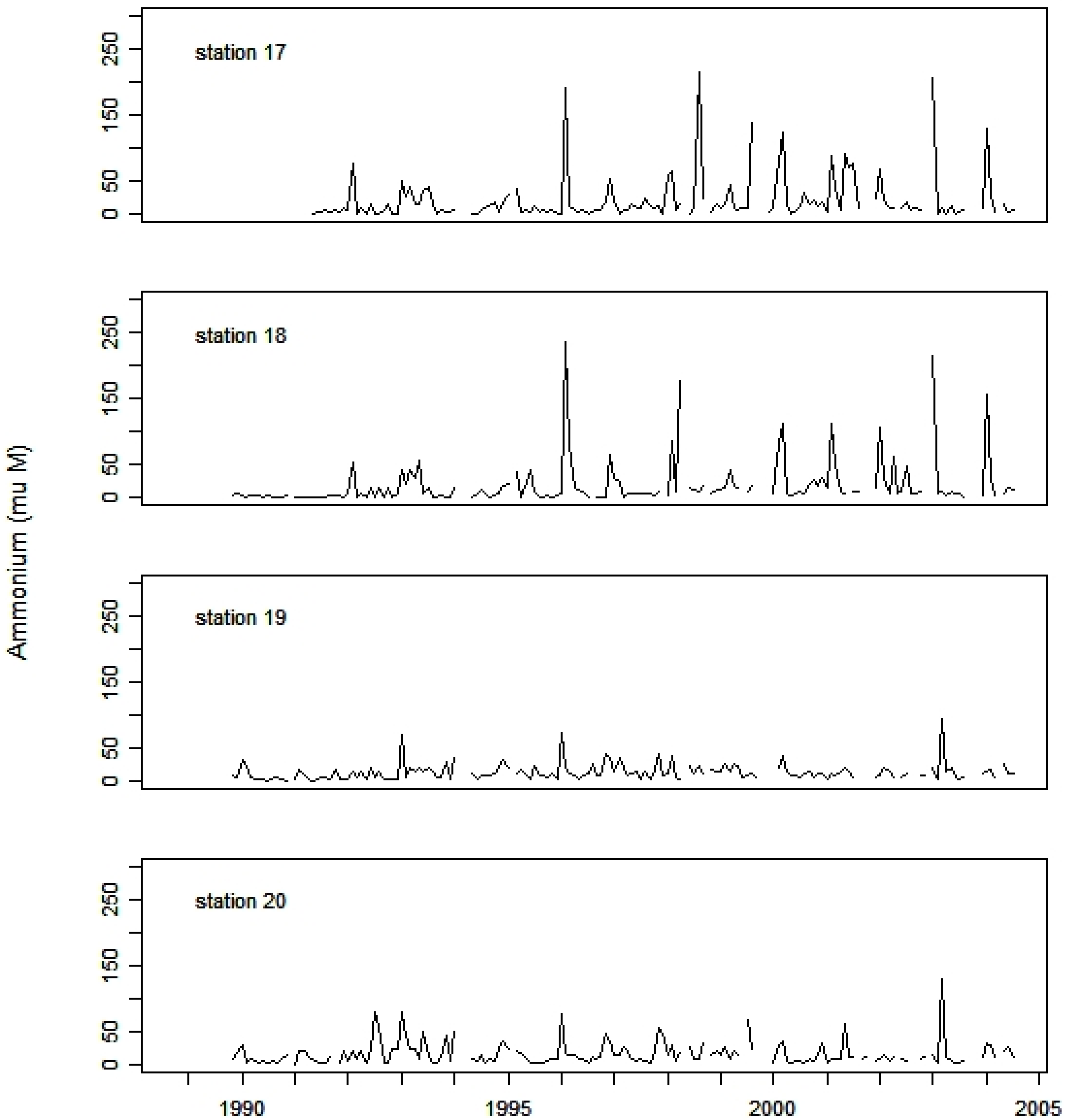

Figure 22. Time Series of Ammonium Concentrations.

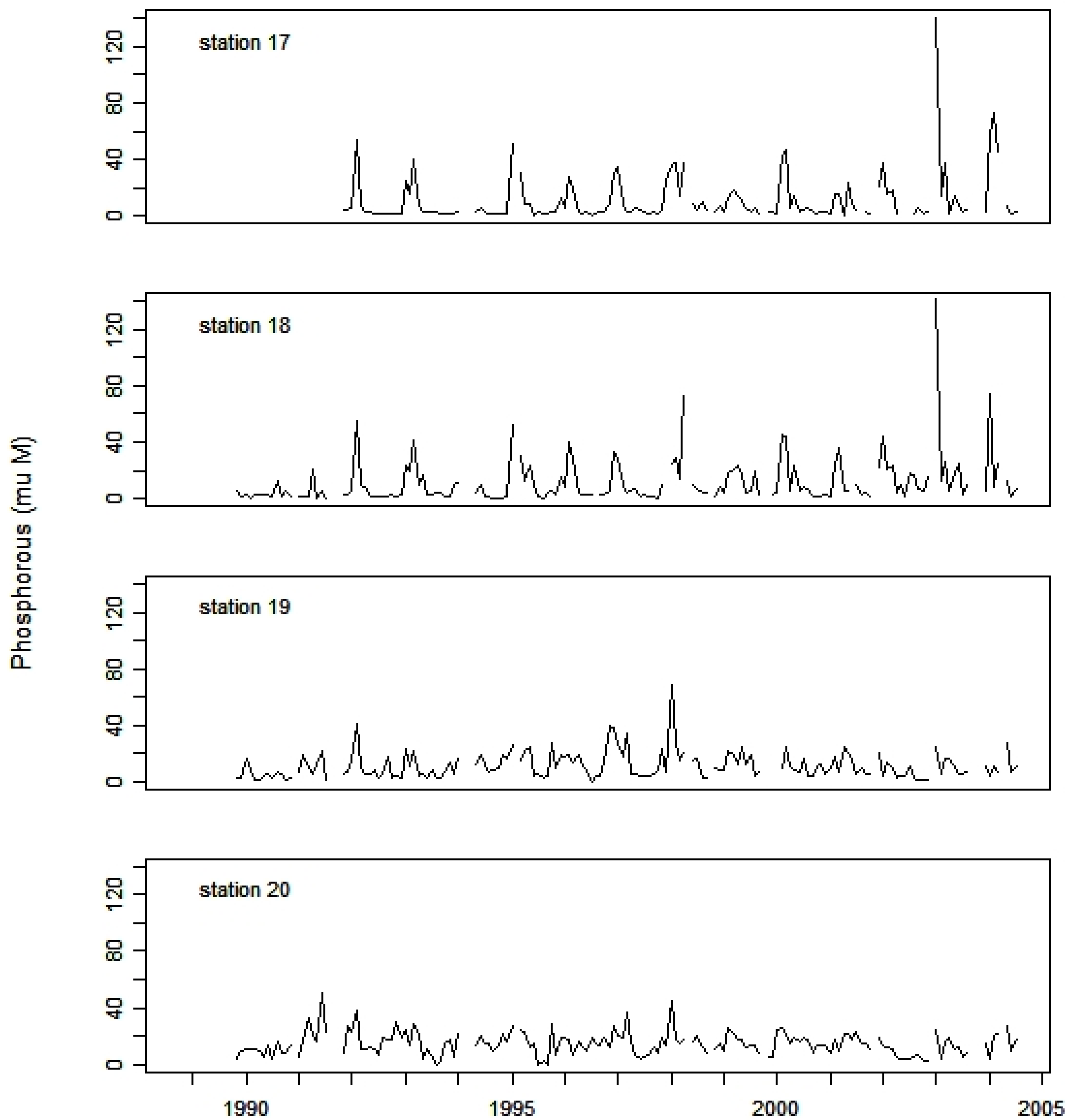

Figure 23. Time Series of ortho-phosphorous concentrations

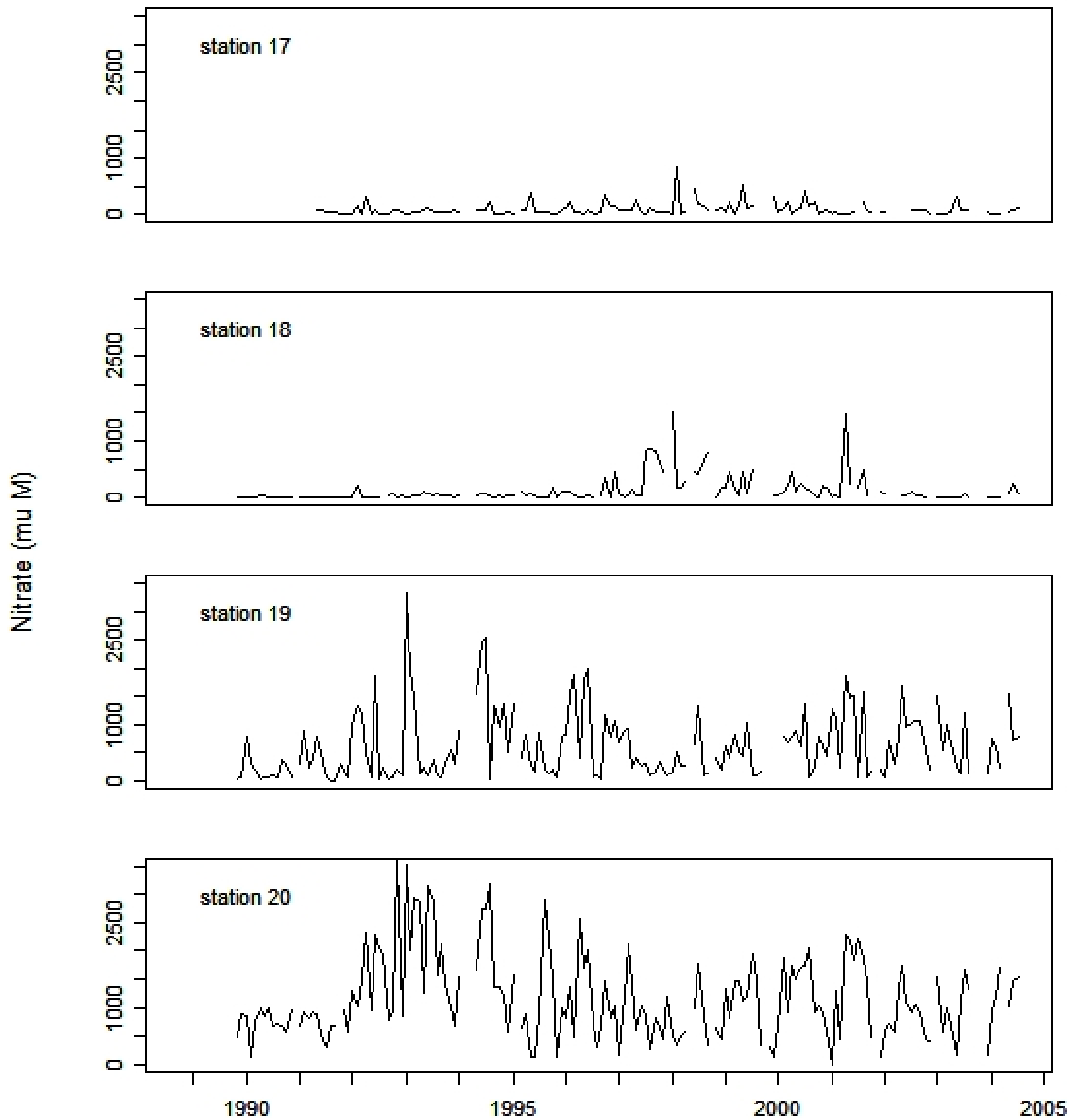

Figure 24. Time Series of Nitrate Concentrations

We expected an annual cycle for most of the observed locations. In Figure 25, monthly boxplots are shown for nitrate, ammonium and ortho-Phosphorous. The plots show some visual evidence of a seasonal cycle. To explore the seasonal trends, we evaluated each station with periodogram to determine if underlying frequencies exists. For example, Figure 21, Bayesian periodogram for Station 18, shows an important annual cycle (12 months), but a shorter six month cycle may also exist. However, annual cycles do not exist for all locations. In some cases, high frequencies were observed and may override importance of the annual cycle.

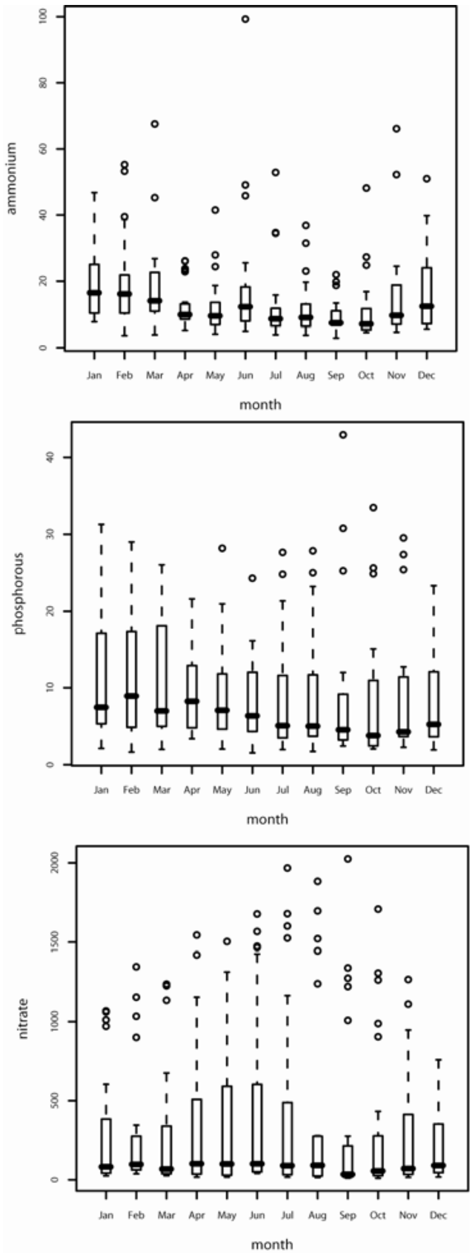

Figure 25. Monthly boxplots for ammonium, ortho-P time, and nitrate series for all locations.

Time Series Models

The objective of this study is to detect and quantify long-term trends in nutrient data. By considering a regression of the log-transformed response on time, we test each of the three variables at each of the 24 stations. We fitted a model consisting of a trend, one harmonic with a yearly cycle and one with a six months cycle using least squares. For all stations, we found that the Bayesian Information Criteria (Schwarz 1978) (BIC) allowed us to discard the model with two harmonics, so only one year harmonic is used throughout the analysis. More explicitly, for each variable and each location, we consider the model

Equation 7

$$\log(Y_t) = \beta_1 + \beta_2 * t + \beta_3 * \cos(2\pi * t/12) + \varepsilon_t + o_t$$

Here t corresponds to months since September 1988, Y_t is either ammonium, ortho-phosphorous, or nitrate, ε_t is a regression error and o_t is an observational error. After fitting the regression using least square error, we observed that the residuals had a correlation structure not corresponding to white noise and was compatible with an autoregressive process. Therefore, we added an autoregressive term

Equation 8

$$\varepsilon_t = \sum \phi_j \varepsilon_{t-j} + \psi_t, \psi_t \sim N\left(0, o_\psi^2\right)$$

This is an important component of the model. In fact, autoregressive processes are stationary and, as such, cannot have any trends. Nevertheless, they can exhibit persistence or quasi-cycles potentially confounded with the actual long-term trend, we are trying to detect. For the observational error o_t, we assume $o_t \sim N(0, o^2_\psi)$ with $o_o > o_\psi$. The former implies the observational variance exceeds the more stable white noise variability in the autoregressive (AR) process. $\tau = 1/\sigma$ and $\tau_o = 1/\sigma_o$ are respectively the precision of ψ_t and o_t.

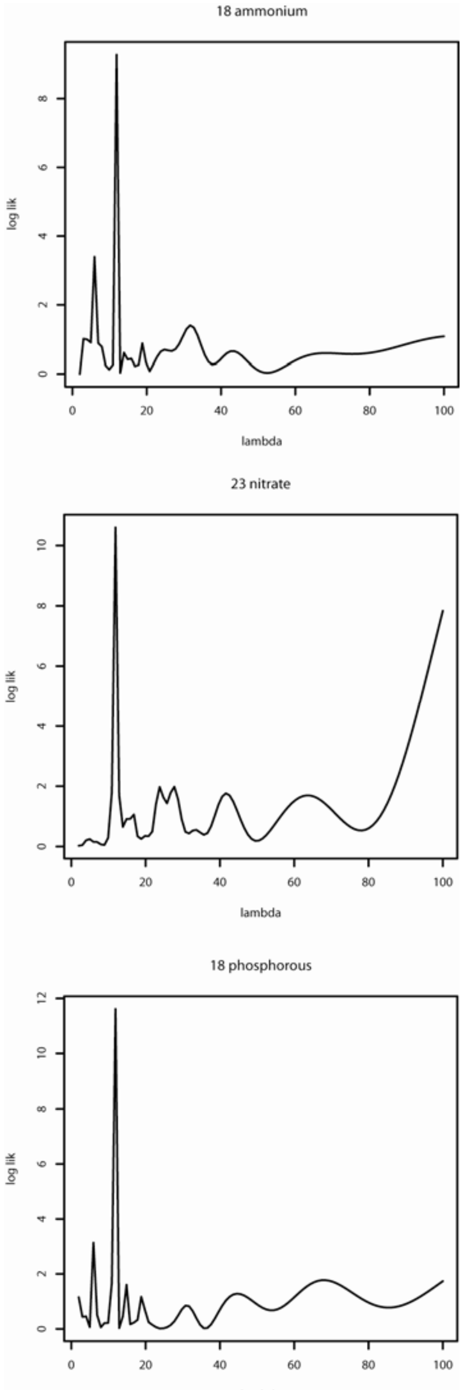

Figure 26. Bayesian Periodogram for ammonium, ortho-phosphorous, and nitrate time series.

Fitting the model

To fit the model in Equation 1, we perform three steps: 1) a model consisting of a trend and a one year harmonic is fitted by least squares. An AR(p) model is fitted to the residuals and the order p of the autoregressive process is selected using again the Bayesian Information Criteria (BIC); and 2) we then fit the model in Equation 1 by generalized least squares. The resulting estimates of $\beta_1,\ldots, \beta_4, \varphi_i$, j = 1, …,p are then used as initial iterates in the next step. In this step, we use the WinBUGS package (Speigelhalter, et al. 2003) to fit the model using a Bayesian approach. WinBUGS uses Markov Chain Monte Carlo (MCMC) methods for the Bayesian inference process. In Bayesian inference, all the information about the unknown model parameters is expressed in terms of the posterior probability distribution. For complex and hierarchical models, this distribution is usually highly dimensional. MCMC methods are algorithms used to get samples from highly dimensional probability distributions. This is achieved by constructing a Markov Chain, which converges after a large number of simulations to an equilibrium distribution. After convergence, the random sequences from the Markov Chain are considered samples from the desired distribution.

From the above procedure we obtain samples from the posterior distributions of the vector model parameters, $\beta_1,\ldots, \beta_4, \tau_\psi, \tau_o$, and φ_j, j =1, …, p. It is possible to assess uncertainties of all parameters since all the information about them is summarized by the joint posterior probability distribution. It is also possible to determine probability intervals, which allow us to quantify the significance of the trends.

To apply the Bayes theorem some prior information is required about the parameters. It is assumed that the joint prior distribution has the following structure:

$$p\left(\beta_1,\ldots,\beta_{4,}\phi_1,\ldots,\phi_p,\tau_\psi,\tau_o\right)=p\left(\beta_1,\ldots,\beta_4\right)p\left(\phi_1,\ldots,\phi_4\right)\cdot p\left(\tau_\psi\right)\cdot p\left(\tau_o\right)$$

where $p(\beta_1,\ldots,\beta_4) \sim N_4(O,B)$ and $p(\varphi_1,\ldots,\varphi_4) \sim N_p(0,\Phi)$, where B and Φ are precision matrices. We assumed that $\Phi \sim$ Wishart(R,p) with scale matrix *R* and degrees of freedom *p*, and *B* is a diagonal matrix with small precision values for the β's (0.0001 to

0.01) in the diagonal. Additionally we assume that τ_ψ follows the rather vague prior $\tau_\psi \sim$ Gamma(0.001,0.001). Finally $\tau_o = \tau_\psi/10$.

Results

Ammonium

Based on the SK test, we generally found the seven sites with increasing concentrations in the southern portion and west end of the slough. Using the Bayesian time series model, we found five out of the 24 locations the ammonium concentration is increasing significantly (locations 12, 14, 15, 18 and 23). Four of these sites also had significant trends using the SK test. In contrast to the SK test, Station 9 did not have a significant long-term trend since the 95% posterior probability interval includes the zero (-0.036, 0.042). However, the mean rate of ammonium increase with respect to the baseline value at the beginning of the measurement period is rather high (285%).

Similarly, the SK test found four sites with declining trend--all of which were also found to be declining with an additional two sites had decreasing ammonium trend (locations 4, 5, 6, 8, 16 and 22). In Table 11, we present the mean rate of change in ammonium concentrations for the whole period of measurements (192 months) and locations, with significant ammonium concentration increase. This rate of change is calculated with respect to the base line. A mean rate of change value of 50% signifies that the nutrient concentration has increased of 50% since the beginning of the measurement period with respect to the baseline. This is calculated as Y_{192}/Y_0 where Y_0 is the initial concentration value and Y_{192} is the concentration at the end of the period. The sites with significant annual seasonal cycle are locations 2, 6, 11, 12, 13, 14, 16, 18, 20 and 24.

Table 10. Percent Increase in Ammonium concentrations for the observations period relative to the baseline.

Site	Mean Change (%)
12	81

14	171
15	140
18	465
23	165

Simulations from the posterior predictive distributions of the logarithm of ammonium under the proposed model were produced by using WinBUGS with the MCMC methods. The results were compared with the observations. Posterior probability intervals corresponding to the 2.5% and 97.5% quantiles from these posterior distribution simulations jointly with the median (50% quantile) were compared with observations at locations 9, 12, 14, 15. Results are presented in Figure 22, which show a very good agreement with observations.

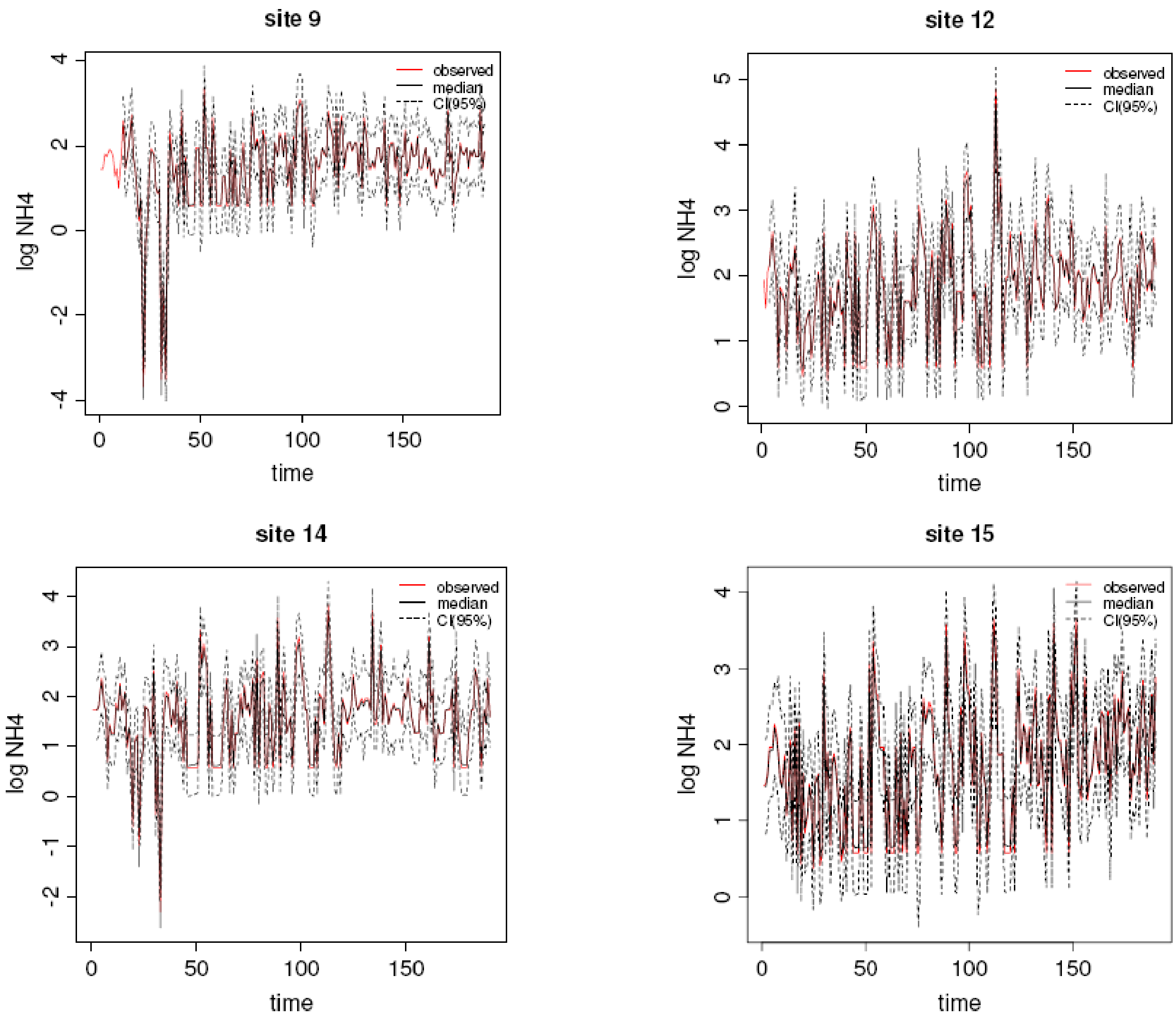

Figure 27. Ammonium time series concentrations comparing observed and modeled.

ortho-Phosphorous

In 4 of the 24 locations the ortho-Phosphorous concentration is increasing (locations 3, 15, 18 and 23), while 5 of the remaining locations have decreasing trends (locations 4, 5, 13, 16 and 20). In Table 11, we present the mean rate of change in ortho-P concentrations, for the whole period of measurements (192 months), for the locations with significant ortho-P concentration increase. As before, this rate of change is calculated with respect to the base line.

The sites with significant annual cycle are locations 12, 14, 16, 18, 19, 20 and 23.

Table 11. Percent Increase in ortho-Phosphorous concentrations for the observations period relative to the baseline.

Site	Mean Change (%)
3	37
15	163
18	200
23	485

As before, posterior predictive distributions for the logarithm of ortho-P were compared with observations now at locations 3, 5, 13 and 15. The results are shown in Figure 23. As before, the agreement between observations and the simulations is satisfactory.

Although the Seasonal Mann-Kendall test is not directly comparable with the time series model fitting approach used in this analysis, it is expected in case of low autocorrelation of the time series, a non-significant trend result with the Mann-Kendal test would yield an equivalent result in the Bayesian analysis.

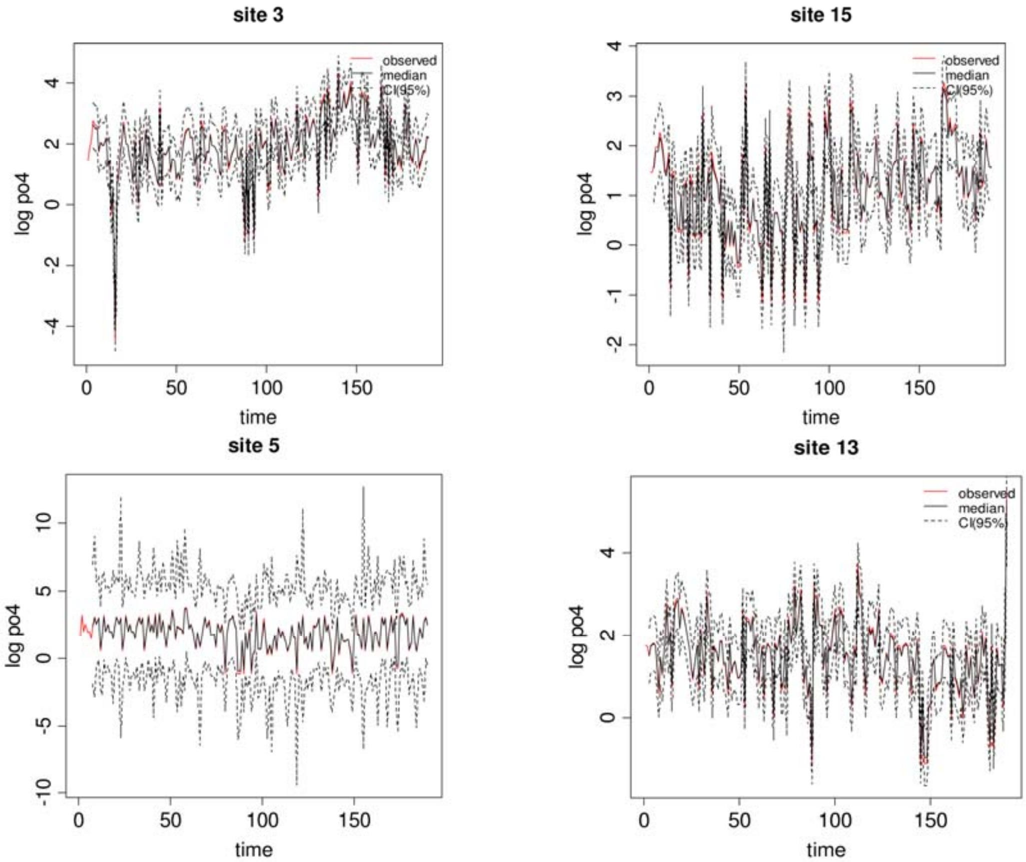

Figure 28. Observed and modeled values of log ortho-P for stations 3, 5, 15, and 13.

Discussion

Elevated nitrogen and phosphorous concentrations in estuarine environments generally associated with anthropogenic sources. Previous papers have demonstrated portions of Elkhorn Slough have high concentrations of nutrients (Caffrey, et al. 1997, Caffrey et al. 2007). However, determining trends is challenging due to the complex hydrology and heterogeneous nature of land use in the slough. Not surprisingly, nutrient concentrations trends are variable across the slough and even in opposite directions. By combining two approaches, we found nutrient concentrations in the slough at some locations are increasing, while others are declining.

There was a strong seasonal component to the nutrient concentrations. The strong twelve month periodicity of the data is consistent with the seasonality of the growing season in the region, agricultural activities, and the Mediterranean climate. The sites with strong seasonality are scattered throughout the slough and hard to make generalizations the cause of periodicity. In general, the sites tend to be tidal, but spatially dependent on freshwater sources. Perhaps, these freshwater sources have stronger seasonality influence. However, adjacent sites or sites with similar characteristics did not have strong twelve month periodicities. For example, Station 20 and 24 both had twelve month periodicities, but Station 21 did not, even though it is within the same region of the slough. Interpreting these data will require detailed understanding of tidal and riverine hydrology of the slough in the context of land use runoff with a spatially explicit hydrologic model.

The locations 4, 5, 8b declined in nitrate concentration over the sampling period. We noted sampling of Station 8b was changed because the marsh filled with sediment. In spite of these declines, six locations increased in concentrations (2, 3, 8a, 15, 18, 19). However, depending on how the treatments of N.D., the results of site 8a are ambiguous.

Depending on the constituent measured and method of analysis, between five and eight locations had increasing nutrient concentrations, however, these two methods did not select the same sites. For example, the Bayesian time series model determined locations 12, 14, 15, 18, and 23 were significantly increasing in ammonium concentrations. The sites in the north-west arm of the slough have a catchment area dominated by agriculture. However, the SK test did not detect a significant trend for location 14 although it has a 140% increase in concentrations and is physically located between locations 12 and 15. While it might be argued the non-parametric test is less powerful, the SK test found location 9 for ammonium significant, while the Bayesian test did not. For this location the order of the autoregressive model for the residuals was quite high (p=11), which might explain why there is a difference in the results.

Several locations have had important land use management changes. In particular Locations 4 and 5, are tidally restricted, thus the water quality is dominated by the catchment land use that drains to these sites. In 1994 site management changed dramatically; row crops that were adjacent to the site were replaced by a vegetative buffer strip over 40 meters in width. Based on these data, the set back has effectively reduced nutrient loading into these sites.

After a fifteen-year sampling time almost between 1/3 and 1/2 of the sites had significant long-term trends. Given the dominance of agriculture adjacent to the slough, we thought more sites would have significant increasing trends. However, because land use has not changed dramatically, nutrient loading may have been relatively constant over the last 15 years. The drivers for water quality vary across the sites include overland runoff (Azevedo Pond South), storm event discharge (Carneros Creek), tidal activity, seasonality, etc. These drivers generate temporally isolated spikes in nutrient concentrations making it difficult to determine general relationships to predict water quality across all the sites. For example, high discharge in Carneros Creek can lead to reduced concentrations at the Carneros site but increased concentrations at the downstream site is usually dominated by tidal flushing. In addition, the lack of nutrient trend may be due to counterbalancing effects: nutrient loading may be increasing in parcels due to expanding intensive agriculture, but decreases in other parcels due to conservation organization efforts or improved efficiency of agricultural practices.

Developing predictive models that capture the variability in nutrient concentrations on a seasonal basis is difficult. Most of the sampling sites had period spikes in nutrient concentrations. In most cases, these limited any predictive modeling used to determine if there are seasonal trends in nutrient concentrations. Furthermore, these spikes generally occurred within limited time periods, often in a single month for the whole season. These spikes correlated with rainfall in some locations, but others had their highest concentrations in the summer months. For example, in the northern portion of the slough, Porter Marsh receives flow from Carneros Creek and small waterway that drains Corncob Canyon, as well as, a small area in the Pajaro Valley. During storm events, Carneros Creek and Corncob Canyon Creek deliver nutrients to the northern portion of Elkhorn Slough. Carneros Creek is a flashy system, and flows and concentrations can change dramatically during storm events (Los Huertos, et al. 2001). When discharge is high in these waterways, nutrient concentrations are generally at their lowest. Thus, the water quality in Porter-Bloomfield Marsh can vary dramatically depending on upstream discharge patterns. We believe the causes behind the spatial variation appear to be both differences in inputs (highest where freshwater inputs greatest) and in amount of tidal flushing in the slough.

Long-term Trends

Elevated nutrient concentrations occurred with increasing odds in the northern portion of the watershed and in several of the south sampling locations. Even with a fifteen-year sampling time, changes in water quality are surprisingly difficult to capture. We believe there are several reasons for this difficulty. First, in general, there have been few land use changes in the last 15 years (in contrast to the previous 15 years); thus, nutrient loading has probably been relatively constant. Second, the drivers for water quality vary across the sites that include overland runoff (Azevedo Pond South), storm event discharge (Carneros Creek), tidal activity, seasonality, etc. These drivers generate temporally isolated spikes in nutrient concentrations that make it difficult to determine general relationships that predict water quality across all the sites. For example, high discharge in Carneros Creek can lead to reduced concentrations at the Carneros site but increased concentrations at the downstream site, usually dominated by tidal flushing.

In some locations, the lack of nutrient trend may be due to counterbalancing causes: increases nutrients loads with intensification of agriculture, and decreasing due to conservation efforts aimed at retiring agricultural lands.

Trend Analysis and Monitoring Recommendations

Even after sixteen years of monitoring, water quality changes are subtle. In the context of a Mediterranean climate, where rainfall is limited to irregularly timed events and are not feasible to capture with regular monthly sampling. Water quality, especially nonpoint sources of pollutants, depends on rainfall in the winter season. Therefore, it is not surprising detecting trends in datasets do not capture one of the main drivers of pollutant loading. Another hydrologic driver possibly driving water quality variation is tidal action. We expect incoming and outgoing tides to play a role in water chemistry at some sites. On going studies have been designed to capture this as a potential driver. However, these studies cannot be linked to each station in the slough where it might be incorporated into a time series analysis. In addition, the presence of missing data undermines the capacity to detect a trend signal. In this study, we substituted missing data with median values, which effectively reduces the power of the analysis. In spite of this approach, there is evidence of nutrient changes in the slough. However, based on our effort to detect long-term trends, we recommend the following to improve chances of detecting long-term changes.

- Maintain monthly sampling during the dry season.
- Add sampling to bracket (before, during, and after) rainfall events to determine, which sites and to what extent sites are influenced by rainfall driven water quality changes. We recommend this be done in collaboration with time series analysis in mind, so that it might be incorporated into a more sophisticated model.
- Add sampling to bracket the influence of tides on water chemistry, with the same goals as above.
- The monitoring program has improved dramatically in the last few years, in particular with the development of a quality assurance and control plan. Maintain a water quality monitoring plan to collect high quality data can be expensive and it is tempting to reduce the number of sites to maintain the program. However, based on our analysis, reducing the number of sites reduces the capacity to tell the complexity of the water quality story in Elkhorn Slough.

Conclusions

Water quality within Elkhorn Slough varies on both temporal and spatial scales. The trends at individual sites are resounding support that monitoring water quality is a sensitive method of tracking ecosystem health. The source of variability, increasing turbidity, and elevated nutrient concentrations remains unknown. The Elkhorn Slough watershed has been influenced by numerous anthropogenic changes; however, the long-term effects are relatively unknown. More research is needed to draw valid conclusions and to better understand this complex system.

Literature Cited

Altun Ö, Saçan MT, Erdem AK. 2007. Water Quality and Heavy Metal Monitoring in the Water and Sediment Samples of the Küçükçekmece Lagoon, Turkey (2002-2003). Environmental Monitoring and Assessment: Earth and Environmental Science, Online First?.

Anderson, D. M., P. M. Glibert, and J. M. Burkholder. 2002. Harmful algal blooms and eutrophication: Nutrient sources, composition, and consequences. Estuaries 25:704-726.

Baden, S. P., L. O. Loo, L. Pihl, and R. Rosenberg. 1990. Effects of Eutrophication on Benthic Communities Including Fish - Swedish West-Coast. Ambio 19:113-122.

Barnes J, Owens JP. 1998. Denitrification and Nitrous Oxide Concentrations in the Humber Estuary, UK, and Adjacent Coastal Zones. Marine Pollution Bulletin 37(3-7): 247-260.

Bauer DE, Gomez N, Hualde PR. 2007. Biofilms Coating Schoenoplectus californicus as Indicators of Water Quality in the Rio de la Plata Estuary (Argentina). Environmental Monitoring and Assessment 133: 309-320.

Bauer DE, Gomez N, Hualde PR. 2007. Biofilms Coating Schoenoplectus californicus as Indicators of Water Quality in the Rio de la Plata Estuary (Argentina). Environmental Monitoring and Assessment 133: 309-320.

Beck, N. G., and K. W. Bruland. 2000. Diel biogeochemical cycling in a hyperventilating shallow estuarine environment. Estuaries 23:177-187.

Benoit P, Gratton Y, Mucci A. 2006. Modeling of Dissolved Oxygen Levels in the Bottom Waters of the Lower St. Lawrence Estuary: Coupling of Benthic and Pelagic Processes. Marine Chemistry 102: 13-32.

Billen G, Garnier J, Fight A, Gun C. 2001. Modeling the Response of Water Quality in the Seine River Estuary to Human Activity in its Watershed Over the Last 50 Years. Estuaries 24(6B): 977-993.

Brown J. 2001. A Review of Marine Zones in the Monterey National Marine Santuary, Marine Sanctuaries Conservation Series MSD-01-2. U.S. Department of Commerce, National Oceanic and Atmosphere Administration, Marine Sanctuaries Division, Silver Springs, MD.

Burkholder, J. M., E. J. Noga, C. H. Hobbs, and H. B. Glasgow. 1992. New Phantom Dinoflagellate Is the Causative Agent of Major Estuarine Fish Kills. Nature 358:407-410.

Caffrey, J. M., T. P. Chapin, H. W. Jannasch, L. J. Coletti, and J. C. Haskins. in press. High nutrient pulses, tidal mixing and biological response in a small California estuary, Elkhorn Slough, CA, USA: variability in nutrient concentrations from hoursly to decadal time scales. Estuaries.

Caffrey, J.M., N. Harrington, and B. Ward. 2002. Biogeochemical processes in a small California estuary. 1. Benthic fluxes and pore water constituents reflect high nutrient freshwater inputs. Marine Ecology Progress Series 233:39-53.

Chapin, T. P., J. M. Caffrey, H. W. Jannasch, L. J. Coletti, J. C. Haskins, and K. S. Johnson. 2004. Nitrate sources and sinks in Elkhorn Slough, California: Results from long-term continuous in situ nitrate analyzers. Estuaries 27:882-894.

Colbert D, McManus J. 2003. Nutrient Biogeochemistry in an Upwelling-Influenced Estuary of the Pacific Northwest (Tillamook Bay, Oregon, USA). Estuaries 26(5):1205-1219.
Dafner EV, Mallin MA, Souza JJ, Wells HA, Parsons DC. 2007. Nitrogen and Phosphorus Species in the Coastal and Shelf Waters of Southeastern North Carolina, Mid-Atlantic U.S. Coast. Marine Chemistry 103: 289-303.
Dai M, Guo X, Zhai W, Yuan L, Wang B, Wang L, Cai P, Tang T, Cai WJ. 2006. Oxygen Depletion in the Upper Reach of the Pearl River Estuary during a Winter Drought. Marine Chemistry 102: 159-169.
Eddy FB. 2004. Review Paper: Ammonia in Estuaries and Effects on Fish. Journal of Fish Biology 67: 1495-1513.
Edgar GJ, Barrett NS, Graddon DJ, Last PR. 2000. The conservation significance of estuaries: a classification of Tasmanian estuaries using ecological, physical and demographic attributes as a case study. Biological Conservation 92(3):383-397.
EPA. 2007. National Estuary Program Coastal Condition Report. no author stated. Site name: National Estuaries Program. http://www.epa.gov/owow/oceans/nepccr/index.html
Ferreira JG, Nobre AM, Simas TC, Silva MC, Newton A, Bricker SB, Wolff WJ, Stacey PE, Sequeira A. 2006. A Methodology for Defining Homogeneous Water Bodies in Estuaries-Application to the Transitional Systems of the EU Water Framework Directive. Estuarine, Coastal and Shelf Science 66: 468-482.
Gabric, A. J., and P. R. F. Bell. 1993. Review of the Effects of Nonpoint Nutrient Loading on Coastal Ecosystems. Australian Journal of Marine and Freshwater Research 44:261-283.
Garnier J, Billen G, Cebron A. 2007. Modeling Nitrogen Transformations in the Lower Seine River and Estuary (France): Impact of Wastewater Release on Oxygenation and N2¬O Emission. Hydrobiologia 588: 291-302.
Gray JS, Wu RS, Or YY. 2002. Effects of Hypoxia and Organic Enrichment on the Coastal Environment. Environmental Science and Pollution Management 238: 249-279.
Hagy JD, Boynton WR, Keefe CW, Wood KV. 2004. Hypoxia in Chesapeake Bay, 1950-2001: Long-term Change in Relation to Nutrient Loading and River Flow. Estuaries 27(4):634-658.
Hansson, L. A., M. Gyllstrom, A. Stahl-Delbanco, and M. Svensson. 2004. Responses to fish predation and nutrients by plankton at different levels of taxonomic resolution. Freshwater Biology 49:1538-1550.
Helsel, D. R., and R. M. Hirsch. 1992. Statistical Methods in Water Resources. Elsevier, New York.
Helsel, D.R., and L.M. Frans. in press. Regional Kendall test for trend. Environmental Science and Technology.
Howarth RW, Sharpley A, Walter D. 2002. Sources of Nutrient Pollution to Coastal Waters in the United States: Implications for Achieving Coastal Water Quality Goals. Estuaries 25(4b):656-676.
Johnston SG, Slavich PG, Hirst P. 205. The Impact of Controlled Tidal Exchange on Drainage Water Quality in Acid Sulphate Soil Backswamps. Agricultural Water Management 73: 87-111.

Kennish, M. J. 2004. NERRS research and monitoring initiatives. Journal of Coastal Research:1-8.
Laprise, R., and J. J. Dodson. 1994. Environmental Variability as a Factor Controlling Spatial Patterns in Distribution and Species-Diversity of Zooplankton in the St-Lawrence-Estuary. Marine Ecology-Progress Series 107:67-81.
Liu Z, Liu X, Liao C. 2007. Daytime Deposition and Nighttime Dissolution of Calcium Carbonate Controlled by Submerged Plants in a Karst Spring-fed Pool: Insights From High Time-resolution Monitoring of Physico-chemistry of Water. Environmental Geology: Online First?
Madden, C. J., and W. M. Kemp. 1996. Ecosystem model of an estuarine submersed plant community: Calibration and simulation of eutrophication responses. Estuaries 19:457-474.
Maes J, Stevens M, Breine J. 2007. Modelling the Migration Opportunities of Diadromous Fish Species Along a Gradient of Dissolved Oxygen Concentration in a European Tidal Watershed. Estuarine, Coastal and Shelf Science 75: 151-162.
Malone TC, Crocker LH, Pike SE, Wendler BW. 1988. Influences of River Flow On the Dynamics of Phytoplankton Production in a Partially Stratified Estuary. Marine Ecology Progress Series 48: 235-249.
Miranda J, Balachandran KK, Ramesh R, Wafar M. 2008. Nitrification in Kochi Backwaters. Estuarine, Coastal and Shelf Science 78: 291-300.
Moyle PB, Cech JJ. 1996. Fishes: An Introduction to Ichthyology, 3rd. New Jersey: Prentice Hall.
Nixon, S. W. 1995. Coastal Marine Eutrophication - a Definition, Social Causes, and Future Concerns. Ophelia 41:199-219.
Nizzoli D, Bartoli M, Cooper M, Welsh DT, Underwood GJC, Viaroli P. 2007. Implications for Oxygen, Nutrient Fluxes and Denitrification Rates During the Early Stage of Sediment Colonisation by the Polychaete Nereis spp. in Four Estuaries. Estuaries, Coastal and Shelf Science 75: 125-134.
Nocker A, Lepo JE, Martin LL, Snyder RA. 2007. Response of Estuarine Biofilm Microbial Community Development to Change in Dissolved Oxygen and Nutrient Concentrations. Microbial Ecology 54: 532-542.
Paz M, Gomez-Parra A, Forja J. 2007. Inorganic Carbon Dynamic and Air-Water CO2 Exchange in the Guadalquivir Estuary (SW Iberian Peninsula). Journal of Marine Systems 68: 265-277.
Pihl, L., S. P. Baden, and R. J. Diaz. 1991. Effects of Periodic Hypoxia on Distribution of Demersal Fish and Crustaceans. Marine Biology 108:349-360.
Price, A. R. G. 2002. Simultaneous 'hotspots' and 'coldspots' of marine biodiversity and implications for global conservation. Marine Ecology-Progress Series 241:23-27.
Rabalais, N. N., W. J. Wiseman, R. E. Turner, B. K. SenGupta, and Q. Dortch. 1996. Nutrient changes in the Mississippi River and system responses on the adjacent continental shelf. Estuaries 19:386-407.
Sanger, D. M., M. D. Arendt, Y. Chen, E. I. Weener, A. F. Holland, D. Edward, and J. M. Caffrey. 2002. A synthesis of water quality data: National Estuarine Research Reserve system-wide monitoring program (1995-2000). National Estuarine

Research Reserve Technical Report Series 2002:3. Department of Natural Resources, Marine Resources Division No. 500, South Carolina.
Serkov VM. 2003. Salinity Tolerance of Some Teleost Fishes of Peter the Great Bay, Sea of Japan. Russian Journal of Marine Biology 29(6): 368-371.
Speigelhalter, D.J., Thomas, A. Best, N.G. and Lunn, D. 2003. WinBugs User Manual (Version 1.4) Cambridge: Mrc Biostatistics Unit, www.mrc-bsu.cam.ac.uk/bugs.
Sunitha MS, Jayaprakas V. 1997. Influence of pH, Temperature, Salinity and Media on Activation of Motility and Short Term Preservation of Spermatozoa of an Estuarine Fish, Mystus gulio (Hamilton) (Siluridae-Pisces). Indian Journal of Marine Science 26: 361-365.
Swartz, G, 1978. Estimating the dimensions of a model. Ann. Stat. 6:461-464.
Tango PJ, Magnien R,Butler W, Luckett C, Luckenbach M, Lacouture R, Poukish C. 2005. Impacts and Potential Effects Due to Prorocentrum minimum Blooms in Chesapeake Bay. Harmful Algae 4: 525-531.
Touchette BW. 2007. Seagrass-Salinity Interactions: Physiological Mechanisms Used by Submersed Marine Angiosperms for a Life at Sea. Journal of Experimental Marine Biology and Ecology 350: 194-215.
Turner RE, Rabalais NN, Justic D. 2008. Gulf of Mexico Hypoxia: Alternate States and a Legacy. Environmental Science and Technology 42: 415-422.
Van Dyke, E., and K. Wasson. 2005. Historical ecology of a central California estuary: 150 years of habitat change. Estuaries 22:173-189.
Wenner, E. L., and M. Geist. 2001. The National Estuarine Research Reserves program to monitor and preserve estuarine waters. Coastal Management 29:1-17.
Whitfield, A. K. 1994. Fish Species-Diversity in Southern African Estuarine Systems - an Evolutionary Perspective. Environmental Biology of Fishes 40:37-48.
Wright DA, Mason RP. 2000. Biological and Chemical Influences on Trace Metal Toxicity and Bioaccumulation in the Marine and Estuarine Environment. International Journal of Environment and Pollution 13: 1-6.
Yüksek A, Okuş E, Yilmaz İN, Aslan-Yilmaz A, Taş S. 2006. Changes in Biodiversity of the Extremely Polluted Golden Horn Estuary Following the Improvements in Water Quality. Marine Pollution Bulletin 52: 1209-1218.
Zhai W, Dai M, Cai WJ, Wang Y, Wang Z. 2005. High Partial Pressure of CO2 and its maintaining Mechanism in a Subtropical Estuary: The Pearl River Estuary, China. Marine Chemistry 93: 21-32.

Appendix 1.

Monthly monitoring and sampling has been carried out at 6 locations since 1988 with additional locations added over the years for a total of 24 sampling locations. Between 1988 and 1994 in-field water quality observations included salinity and temperature (YSI model 33, Marion MA), dissolved oxygen (YSI model 57, Marion MA), pH (Orion model 211, Marion MA), turbidity (Moniteck model 21 PE, *city*). Starting in 1994 to 2000, water quality parameters were monitored with a Solomat multiprobe (803PS Sonde, Norwalk, CT). Beginning December 2000 an YSI multiprobe (model 6000) and added a chlorophyll probe. All sensors were calibrated with appropriate standards following manufacturer recommendations prior to each sampling trip.

Temperature measurements were made with YSI multiprobe sensors using thermistor technology. The accuracy of temperature measurements is 0.15% with a resolution of 0.01%. Temperature thermistors are very reliable and require no calibration or maintenance (YSI, Series 6 Owners Manual, 069300B). They exhibit less than 0.01% drift that is usually associated with a change in the thermistor resistance. Thermistor drift is generally caused by exposure to high temperatures, i.e. well outside the range of values in estuarine environments. This information is important to exclude the possibility that the observed trends are due to equipment malfunction.

Grab samples were collected in clean polypropylene or polyethylene bottles 10 cm from the water surface and transported to the laboratory for analysis in coolers. Nutrient analysis (nitrate, ammonium and inorganic phosphate) was performed by the Monterey Bay Aquarium Research Institute between 1988 and 1991. Samples were centrifuged to remove any sediment and then run on a flow injection analyzer, (Alpkem, Series 300, OI Analytical, College Station, TX) within 48 hours of collection. Standard wet chemistry techniques were used, cadmium reduction for nitrate, phenol-hyperchlorate for ammonium, and ascorbic acid-molybdate for inorganic phosphate (Strickland and Parsons, 1972).

Beginning in December of 1991 the Monterey County Consolidated Chemistry Laboratory processed and analyzed the samples for nutrient concentrations. Samples were immediately filtered (0.45 micron GFF) and were immediately analyzed or frozen and analyzed later. Nitrate (EPA 300.0) and dissolved inorganic phosphate (SM 4500 P E) were analyzed using ion chromotography (Dionex, ICS-90, Sunnyvale, CA). Ammonia concentrations were analyzed using an ion selective probe (SM 4500 NH_3 F) (APHA 1989). Samples are filtered through Dixonex OnGuard filters to remove tannins, chloride, and silver precipitate (which may occur during filtration through Ag filter) prior to analysis to reduce interference. Samples were diluted when concentrations exceeded the linear portion of the standard curve. Starting in 1991 nutrient analysis at the county lab was done…

Table 1. Field Equipment and Laboratory Methods (need to dig to see if I can find old field equipment ranges)

Parameter	Laboratory	Equipment / Method	Range/Method Detection Limit
Temperature			
1988 – 1994		YSI 33	
1994 – 2000		Solomat 803PS	
2000 – 2004		YSI 6000 series	⁻5 – 45 ºC
Salinity/Conductivity			
1988 – 1994		YSI 33	
1994 – 2000		Solomat 803PS	
2000 – 2004		YSI 6000 series	0 – 70 ppt, 0 – 100 mS/cm
Dissolved Oxygen			
1988 – 1994		YSI 57	
1994 – 2000		Solomat 803PS	
2000 – 2004		YSI 6000 series	0 – 500% air saturation, 0 – 50 mg/L
pH			
1988 – 1994		Orion 211	
1994 – 2000		Solomat 803PS	
2000 – 2004		YSI 6000 series	2 – 14 standard units
Turbidity			
1988 – 1994		Moniteck 21 PE	
1994 – 2000		Solomat 803PS	
2000 – 2004		YSI 6000 series	0 – 1000 NTU
Nitrate-N			
1989 – 1991	MBA[1]	Strickland and Parsons 1972	Not recorded
1991 – 1992	MCCCL[2]	Not recorded	0.002 – 0.011 mg N / L
1993 – 1996	MCCCL[2]	SM4500-NO_3 E	0.226 mg N / L
1997 – 2004	MCCCL[2]	EPA 300.0	0.018 – 0.226 mg N / L
Ammonium-N			
1989 – 1991	MBA[1]	Strickland and Parsons 1972	Not recorded
1991 – 1992	MCCCL[2]	Not recorded	0.05 – 0.10 mg N / L
1993 – 2004	MCCCL[2]	EPA 350.3	0.05 mg N / L
Orthophosphorous-P			
1989 – 1991	MBA[1]	Strickland and Parsons 1972	Not recorded
1991 – 1992	MCCCL[2]	Not recorded	0.02 – 0.03 mg P / L
1993 – 2004	MCCCL[2]	SM 4500 PE, EPA 365.2	0.02 – 0.03 mg P / L

[1]Monterey Bay Aquarium
[2]Monterey County Consolidated Chemistry Laboratory